SSCL-SR-1055

Superconducting Super Collider Laboratory

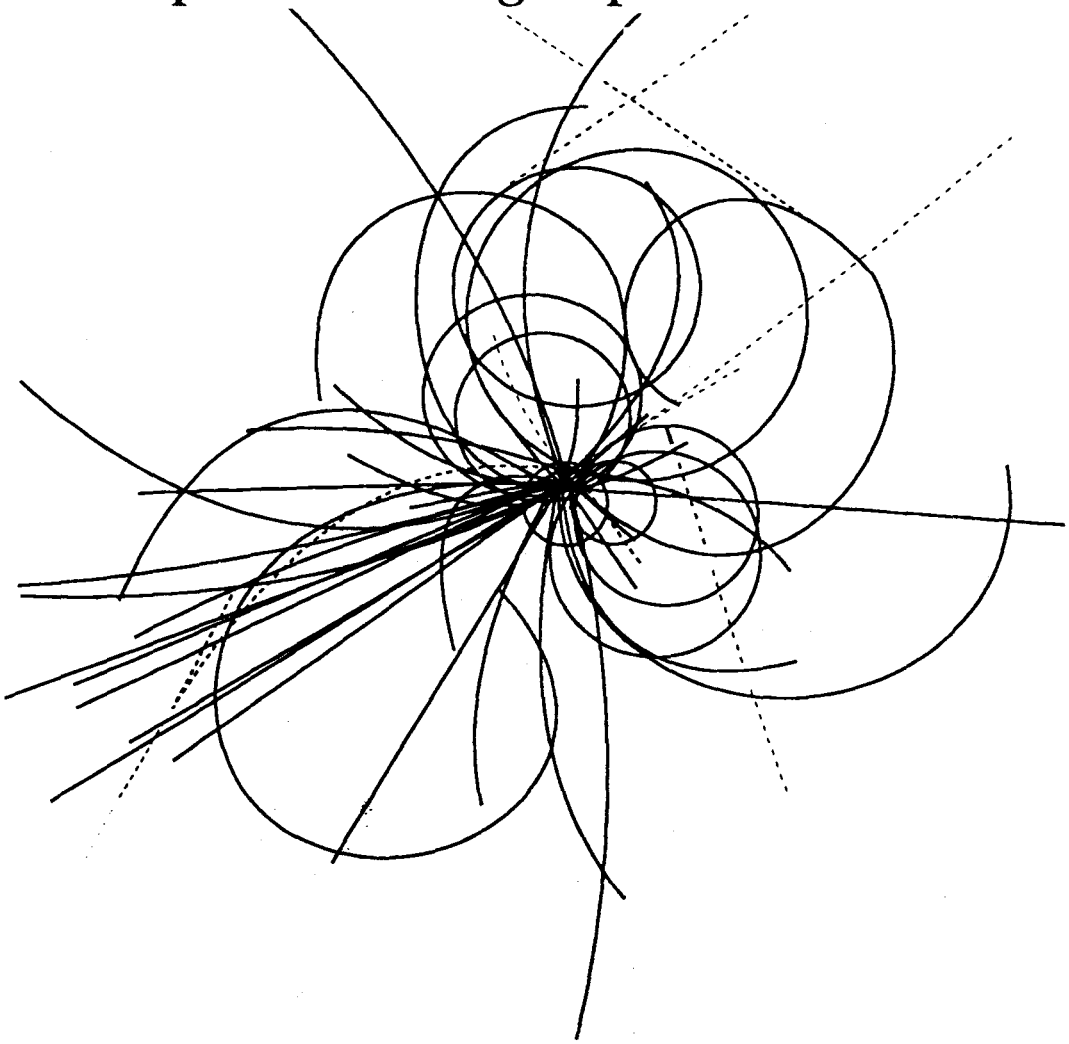

Site-Specific Conceptual Design Executive Summary

July 1990

Site-Specific Conceptual Design of the Superconducting Super Collider

Executive Summary

Material prepared by the staff of the SSC Laboratory

M. G. D. Gilchriese and K. Metropolis

Editors

Superconducting Super Collider Laboratory*
2550 Beckleymeade Avenue
Dallas, Texas 75237

July 1990

*Operated by Universities Research Association, Inc. under contract no. DE-AC02-89ER40486 with the U.S. Department of Energy.

Contents

1. Introduction 1

2. Physics at the SSC
   - 2.1 Why Do We Need the SSC? 4
   - 2.2 Physics Concepts at SSC Energies 5
   - 2.3 Discovering New Physics 6
   - 2.4 Further Studies of the Standard Model 7

3. The Project and Site
   - 3.1 Origins of the SSC 8
     - 3.1.1 The SSC Concept 8
     - 3.1.2 The Early Conceptual Design 8
     - 3.1.3 Selection of the Site 9
     - 3.1.4 Formation of the SSC Laboratory 9
     - 3.1.5 Reviews of Design Energy and Luminosity 9
     - 3.1.6 The SSC Laboratory Today 10
   - 3.2 Description of the Site and Collider Tunnel 12
   - 3.3 Environmental Impact 16

4. The SSC Research Complex
   - 4.1 A Reliable, Flexible Design 17
   - 4.2 The Accelerator Complex 17
     - 4.2.1 Overview of the Accelerators 17
     - 4.2.2 Design Parameters 20
     - 4.2.3 Technical Components 28
   - 4.3 Experimental Systems 36
     - 4.3.1 Introduction 36
     - 4.3.2 Experiments at the SSC 36
     - 4.3.3 Interaction Regions 39
     - 4.3.4 Experimental Plant and Utility Requirements 40
     - 4.3.5 Test Beams 43

5. Operations
   - 5.1 Operations Cycles 45
   - 5.2 Future Options 45
     - 5.2.1 Beam Bypasses 47
     - 5.2.2 Experiments Beyond the Initial Complement 47
     - 5.2.3 Increased Luminosity 47

6. Project Status and Outlook
   - 6.1 Goals of the Next Two Years 51
   - 6.2 Cost Summary 52
   - 6.3 Schedule Summary 53

References 55

List of Illustrations 57

List of Tables 59

1. Introduction

The Superconducting Super Collider (SSC) will be the world's largest and most energetic particle accelerator. It is designed to explore the basic structure and behavior of matter and energy at distance scales far smaller than is possible with existing or planned instruments. The size and energy of the SSC were chosen to address some of today's deepest physics questions raised by the successful yet incomplete theories of the underlying structure of all matter and to view far beyond our current horizons of knowledge in this scientifically exciting and historically important area of science.

To build the SSC and to provide the center for exploiting its scientific promise, the SSC Laboratory was established. The SSC Laboratory has two principal goals or objectives: to create a premier international high-energy physics laboratory by the year 2000 and to create an international resource for all levels of scientific education.

Reaching the first goal will depend on many factors. The laboratory will plan, construct, and operate high quality accelerator and detector systems in a timely manner, which will involve establishing and maintaining technical requirements for the accelerator as well as establishing and meeting schedule and cost objectives. This quality and reliability will facilitate the full use of the laboratory's technical resources by the scientific community. Program flexibility and future upgrade potential will be provided to assure an aggressive and successful response by the laboratory to new scientific opportunities. A key to success is the laboratory staff: the laboratory will recruit outstanding scientists, engineers, and others, who will be encouraged to pursue innovative research in areas relevant to the laboratory's mission.

The second goal—creating an educational resource—will require the SSC Laboratory to promote and encourage the use of the laboratory and its facilities in both construction and technology. As a corollary, laboratory staff will be provided with opportunities to participate in educational activities at all levels, including pre-college, undergraduate, and graduate science education and training. On a more basic level, information on broad areas of science will be provided to the general public.

The SSC will be a 20 TeV $\times$ 20 TeV proton-proton collider with a design luminosity of 10^{33} cm^{-2} sec^{-1}, yielding more than 10^8 interactions per second. It is designed to achieve collisions between the fundamental constituents of matter at energies of about 1 TeV, the energy scale at which theory predicts new phenomena crucial to an understanding of the fundamental interactions will arise. Figure 1.1 shows a schematic layout of the SSC complex. The initial configuration of the SSC will include four interaction regions for experiments. Four more interaction regions, located in beam bypasses in both the west and east sides of the ring, may be added as part of a future upgrade. In addition, the potential for increasing the peak luminosity of the SSC to above 10^{34} cm^{-2} sec^{-1} is being evaluated.

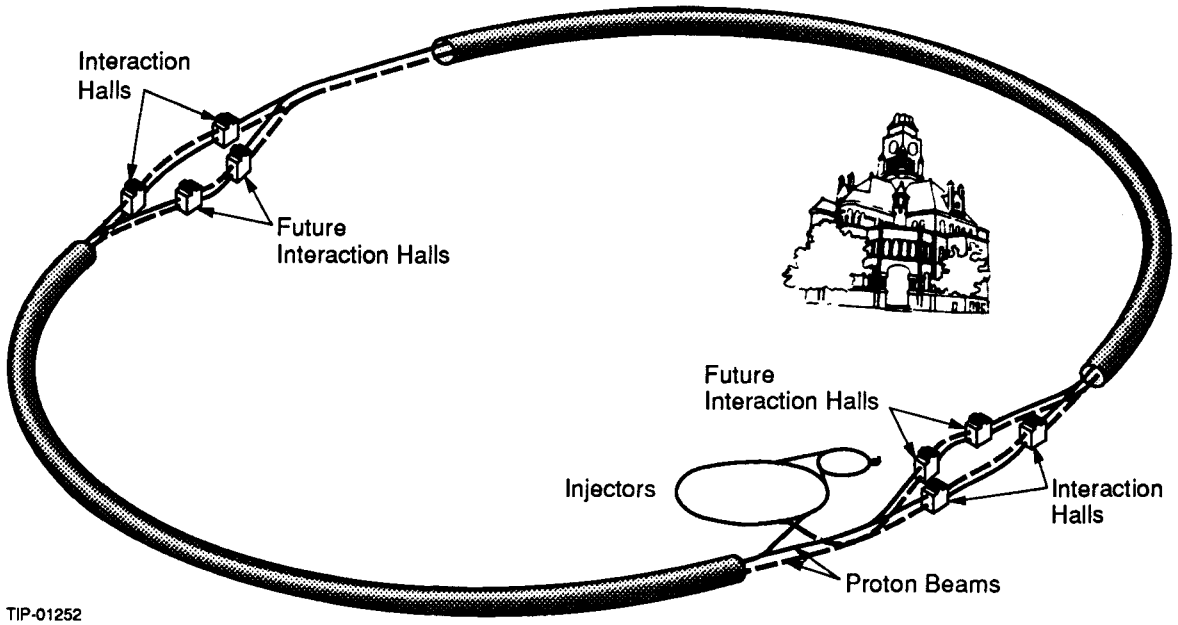

Figure 1.1 A schematic layout of the SSC. The black squares indicate the initial interaction regions. The dotted lines indicate future beam bypasses, which would make possible up to four additional interaction regions.

The SSC will be a unique scientific instrument for exploring the frontiers of particle physics. No other planned or existing accelerator is capable of investigating as many aspects of the fundamental constituents of matter and searching as extensively for new phenomena. A broad program of research is expected to extend for decades.

Research at the SSC will be open to all interested physicists from all countries. It is expected that there will be substantial opportunities for governments and skilled and creative researchers from around the world to contribute to both the accelerator and the detectors.

This document summarizes the physics motivation of the SSC as well as its history and current status. Only a simple summary of the SSC costs and schedules is provided here. A more detailed description of the SSC may be found in the Site-Specific Conceptual Design Report (SCDR), which contains a complete description of the SSC accelerator and conventional systems, and in its companion volumes, which provide cost estimates and schedules for the accelerator and other systems.[1]

For more than a decade, particle physicists have recognized that exploring interactions of the fundamental constituents of matter at energies of about 1 TeV is crucial to advancing understanding. The existing standard model of elementary particle physics elegantly synthesizes the observed behavior of elementary particles, but it is not complete. For example, the spontaneous symmetry breaking of the electroweak gauge symmetry, the existence of similar generations of quarks and leptons, and many other vital issues cannot be explored satisfactorily until experiments are carried out at the 1-TeV scale. The energy and luminosity of the SSC have been chosen to allow a detailed exploration of this richly promising energy regime. The physics motivation for the SSC is sketched in Chapter 2.

The only currently practical means for reaching the TeV scale for collisions of the fundamental constituents is with a hadron collider. The evolution of the SSC concept is outlined in Chapter 3.

The design of the SSC accelerators is based both on a well-founded theoretical description of the behavior of high-energy charged-particle beams and on experience gained in the successful construction and operation of the Fermilab Tevatron, the first superconducting synchrotron. The physical scale of the SSC is larger than the Tevatron by more than an order of magnitude, and, as a result, controlling the cost of the SSC without sacrificing performance goals has required detailed design studies and significant research and development, particularly for the superconducting magnets and other collider systems. The results of this work, along with brief descriptions of SSC accelerator systems, are given in Section 4.2.

To detect the results of the collisions at the SSC, sophisticated experimental apparatus will be required. Detectors must sift through the 10^8 high-energy collisions that will take place each second (at design luminosity) and identify and record the collisions of interest. The largest detectors at the SSC will be bigger and more complex than any detector now in operation. Planning for these detectors and for the research program at the SSC has begun. Section 4.3 explains how the experimental program will be planned and how the requirements for experimental support facilities have been estimated.

Prospects for future modifications to the SSC, including beam bypasses and increased luminosity, are discussed in Chapter 5.

Chapter 6 presents an overview of the SSC project today and sets forth the most important goals for the next two years.

2. Physics at the SSC

2.1 Why Do We Need the SSC?

Over the past two decades, enormous advances have been made in our understanding of elementary particles and the forces that govern their interactions. Today we recognize four forces: gravitational, strong, electromagnetic, and weak. The construction of a gauge theory unifying the electromagnetic and weak forces that has not been contradicted by any experimental evidence, together with the existence of a gauge theory for the strong interactions, makes it appear plausible that one day all the forces may be understood as manifestations of a single, unified force. Three kinds of elementary particles have been identified: the quarks and leptons that make up matter and the gauge bosons that carry the forces. The gauge bosons include photons, the carriers of the electromagnetic force, W and Z bosons, the carriers of the weak force, and gluons, the carriers of the strong force.

The quarks and leptons may be arranged in three generations, as shown in Figure 2.1.1. Except for the mass and lifetimes of the particles, the corresponding particles in each generation have similar properties. All but two of the particles have been observed in experiments. The tau neutrino has not yet been observed directly, nor has the top (or t) quark yet been observed although the search for the top quark has shown its mass to exceed 90 GeV. If it is sufficiently massive, its discovery will require energies that the SSC will provide.

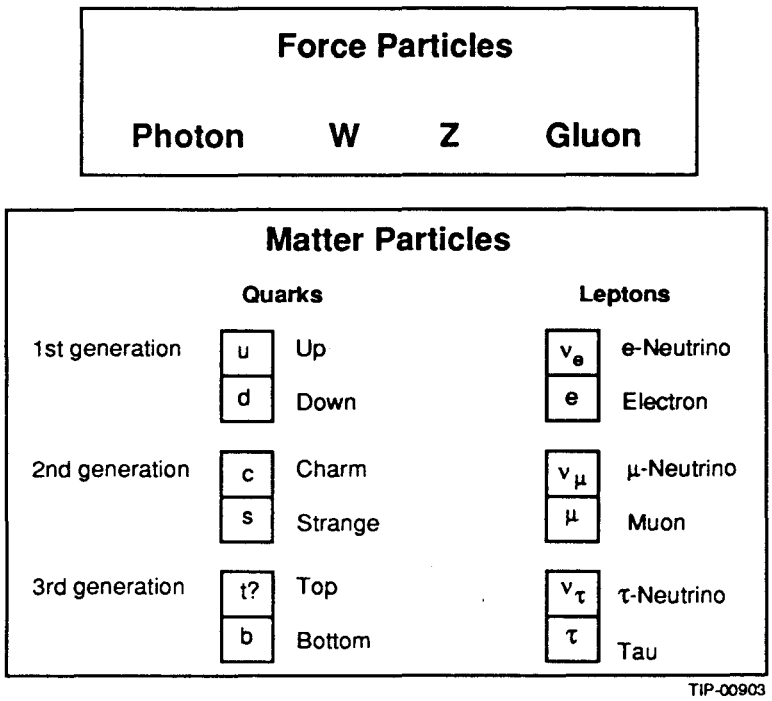

Figure 2.1.1 The particles of the standard model.

Current understanding of the particles and the forces that act on them is summarized in the standard model of elementary particle physics. No convincing experimental evidence exists that contradicts the predictions of this model. Nevertheless, the model is not complete, and many fundamental questions remain unanswered: Are quarks and leptons themselves made up of more fundamental constituents? Are there new forces? What accounts for the different masses of the seemingly fundamental particles?

It is the consensus of the particle physics community that these questions can only be addressed with collisions between the fundamental particles at an energy on the order of 1 TeV—energies not achievable at existing accelerators. The energy and luminosity of the SSC will allow thorough exploration of the energy domain where theory predicts that new phenomena will illuminate the outstanding issues.

In addition, the SSC will be a copious source of known particles that will be important both for testing the standard model and for measuring backgrounds. Studies of rare decays of particles that contain the b or t quark may also point the way to new physics discoveries.

2.2 Physics Concepts at SSC Energies

A proton circulating in the SSC collider may be thought of as a vehicle carrying its quarks and gluon constituents. When two protons collide, there is some probability that constituents of each proton will themselves interact, as shown in Figure 2.2.1. The collision of these constituents at high energy will be a primary focus of SSC experiments. The chance of such collisions occurring depends on the type of constituents involved and on the energy of their collision. Although the protons in the SSC collider rings will have a definite energy of 20 TeV—more than 20 times greater than the most powerful existing machine can provide—a proton's energy is shared among its constituents. The energy of the constituents varies, but each typically carries only a small fraction of the total proton energy. Therefore, a constituent collision with a large fraction of the total energy is less probable than a collision with a smaller fraction of the total energy. To produce statistically significant yields of interesting events, it is necessary to accelerate protons to an energy about 20 times greater than the energy of interest and to have beams intense enough to collide the constituents with sufficient frequency. The SSC design luminosity of 10^{33} cm^{-2} sec^{-1}, several hundred times greater than that of the largest hadron collider today, will yield about 10^8 interactions per second.

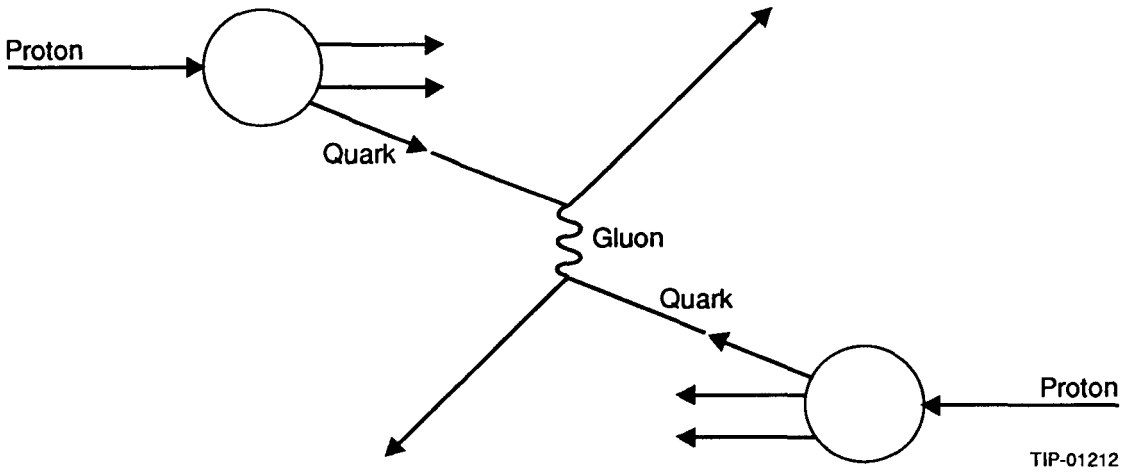

Figure 2.2.1 Interaction of proton constituents. Here a quark from one proton interacts with a quark from another proton.

2.3 Discovering New Physics

The discovery potential of the SSC has been explicated in detail in many places;[2] only the briefest summary will be given here. A major goal of the SSC is to discover the origins of electroweak symmetry breaking, one of the key issues at the frontier of high energy physics. In the context of the standard model, particles acquire mass through the process of electroweak symmetry breaking. The simplest theoretical picture predicts the existence of a massive neutral particle, the Higgs boson, as a consequence of spontaneous symmetry breaking. If indeed this is the case, the Higgs boson could be discovered at the SSC—for example, as a resonance in the invariant mass distribution of Z boson pairs, as shown in Figure 2.3.1.

Other models of electroweak symmetry breaking postulate the existence of more than one kind of Higgs particle or even completely new classes of particles, such as supersymmetric or technicolor particles. In any case, even if a Higgs boson with appreciably lower mass were found tomorrow, exploration of the 1-TeV/c^2 mass region would be of fundamental importance, as outlined below.

The SSC will also be able to search for new gauge bosons—indicating the existence of hitherto-unseen forces in nature—up to a mass of about one-quarter of the total available energy in the proton-proton collisions. The neutral member of this new particle family would be revealed by its decay into electron-positron or muon pairs and would be easy to observe. An example is shown in Figure 2.3.2 for a hypothetical new 4-TeV/c^2 neutral boson.

Although no evidence exists that quarks or leptons have internal structure, it is natural, given the variation in their masses, to ask whether they are truly fundamental. At the SSC it will be possible to have quarks collide with other quarks to discover or limit their substructure, just as the analogous experiments of Rutherford in the early part of this century revealed the existence of the nucleus within the atom, and electron-proton scattering experiments in

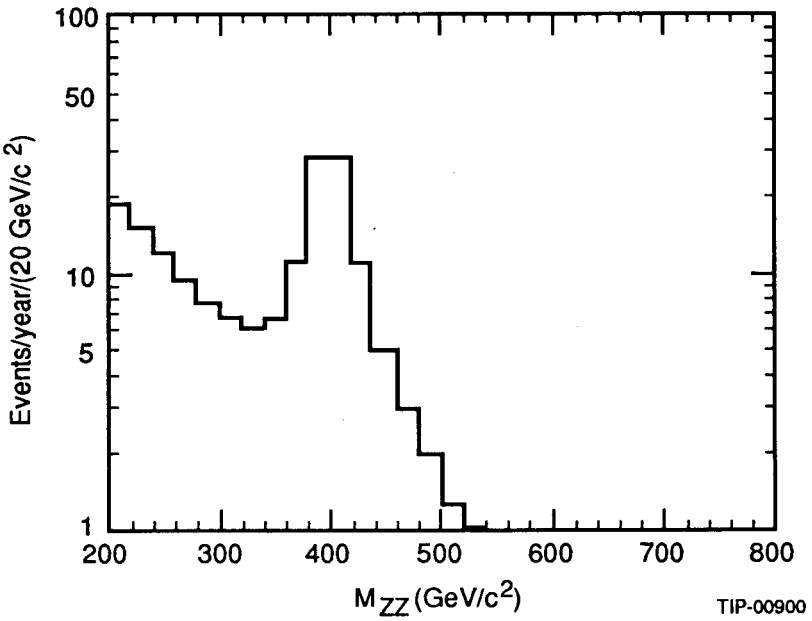

Figure 2.3.1 The invariant mass distribution of Z–boson pairs that would be observed if there is a 400-GeV/c^2 Higgs boson. (The distribution also includes events from background sources other than the Higgs boson decay.)

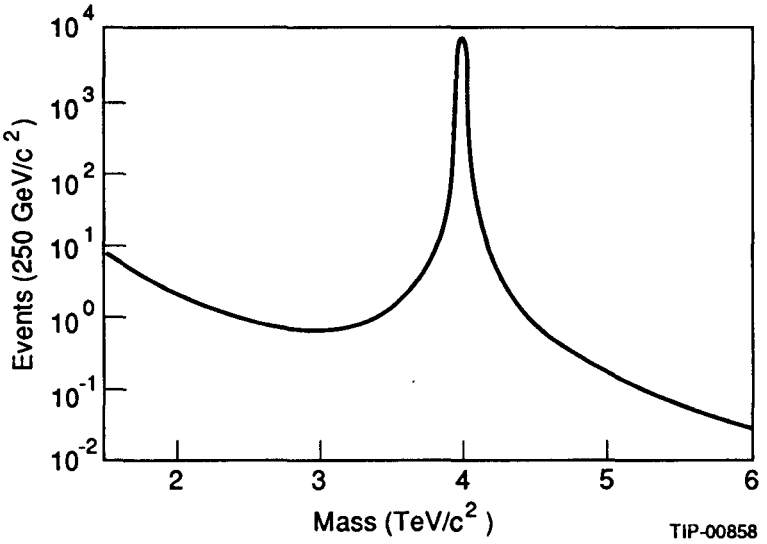

Figure 2.3.2 The observation of a new neutral gauge boson decaying into an electron-positron pair and muon pairs for a boson mass of 4 TeV/c^2.

the 1960s and 1970s provided evidence for quarks within the proton and neutron. At the SSC it will be possible to probe for quark substructure at an energy scale of about one-half the total collision energy.

Some theorists have conjectured the existence of a new set of elementary particles—supersymmetric particles—that are identical to known quarks, leptons, and gauge bosons except for a difference in spin of one-half unit. If this theoretical speculation were to prove correct, an entirely new form of matter could be produced and studied at the SSC.

Some phenomena will have unmistakable signatures—such as the production of a new Z boson and its subsequent decay into an electron and a positron—and could be discovered after the production of only a few events. Other phenomena may be partially obscured, requiring the observation of many hundreds or thousands of events to obtain a statistically significant signal.

2.4 Further Studies of the Standard Model

In addition to new particles, the SSC will produce known particles, in many cases at enormous rates. Detailed studies of the processes that produce such particles are required to verify the predictions of the standard model. Equally important, such work would provide experimental measurements of background processes that may tend to conceal new phenomena.

Detailed studies of the properties of b- and t-quark decays will also be possible with the SSC. At the design luminosity, tens of millions of t-quarks and more than one trillion b-quarks will be produced each year. Sophisticated experiments can exploit this enormous rate of production.

3. The Project and Site

3.1 Origins of the SSC

Although the scientific motivation for studying collisions of the fundamental constituents of matter at high energies emerged more than a decade ago, developing a technically reliable and cost-efficient design for an accelerator that could produce such collisions has required the skill, hard work, and imagination of many people in the intervening years. The result of this dedicated effort is the SSC.

3.1.1 The SSC Concept

The International Committee on Future Accelerators sponsored workshops in 1978 at Fermilab and in 1979 at CERN to explore possibilities for very-high-energy accelerators. A number of approaches were considered, including multi-TeV hadron-hadron colliders. Encouraged by the successful domestication of superconducting accelerator magnet technology for the Fermilab Tevatron, the idea of a Superconducting Super Collider was conceived at the 1982 Summer Study on Elementary Particle Physics and Future Facilities organized by the Division of Particles and Fields of the American Physical Society. Studies of various accelerator and detector issues at Cornell University and at Lawrence Berkeley Laboratory the following year confirmed the viability of the SSC concept.

3.1.2 The Early Conceptual Design

In 1984, after a Reference Designs Study (sponsored by the United States Department of Energy and the directors of the high-energy physics laboratories in the United States) had set forth three technically feasible approaches to achieving 10^8 collisions per second in a collider with 20-TeV proton beams, SSC research and development was formally begun. The Department of Energy contracted with the Universities Research Association, Inc. (a consortium of leading research universities in the United States and Canada that had been organized to build and operate Fermi National Accelerator Laboratory) to oversee the conceptual design of the SSC to be built at a site to be chosen later. Universities Research Association (URA) established the SSC Central Design Group and appointed Professor Maury Tigner of Cornell University as Director. He assembled a group of experts from universities and laboratories around the world, and, as guests of the Lawrence Berkeley Laboratory, the team began their task, with the assistance of Brookhaven National Laboratory, Fermi National Accelerator Laboratory (Fermilab), Lawrence Berkeley Laboratory, Texas Accelerator Center, and American industry.

In March 1986, a Conceptual Design Report was completed. That summer the Department of Energy and independent experts validated the design's feasibility and cost estimate. In January 1987, President Reagan declared the SSC an important national goal.

3.1.3 Selection of the Site

The Department of Energy invited SSC site proposals in April 1987. With the help of a panel from the National Academies of Sciences and Engineering, the forty-three proposals received were reduced to eight, and in November 1988 the Department announced that a site in Ellis Country, Texas, had been chosen.

3.1.4 Formation of the SSC Laboratory

In January 1989, the Department of Energy announced the selection of the URA with two industrial partners, EG&G Intertech and Sverdrup Corporation, to manage the design, construction, and research program of the SSC Laboratory. URA then appointed Professor Roy Schwitters of Harvard University as Director of the SSC Laboratory.

Office space was rented in Dallas, and work began near the site in March 1989. The immediate goals were to provide a conceptual design of the SSC precisely suited to the features of the Texas site, to begin defining the research program, and to build up the SSC Laboratory staff in order to accomplish detailed design and construction of the SSC components. The final conceptual design of the SSC is reported in the Site-Specific Conceptual Design Report (July 1990) and its associated documents.

In September 1989 the United States Congress appropriated $225 million for beginning construction of the SSC.

3.1.5 Reviews of Design Energy and Luminosity

The capability for discovering new physics at a hadron-hadron collider like the SSC is determined by the collision energy and the integrated luminosity, as well as by the capabilities of the detectors. The energy and luminosity specifications for the collider are based on extensive studies of physics goals and accelerator and detector technologies. The tradeoff between energy and luminosity has recently been reviewed in considerable detail by an Ad Hoc Committee on SSC Physics convened by the Director of the SSC Laboratory[3] and by a High Energy Physics Advisory Panel (HEPAP) subpanel.[4] Both groups reaffirmed the need to maintain the original design's beam energy of 20 TeV and luminosity of 10^{33} cm^{-2} sec^{-1}.

The design luminosity, which can be achieved with confidence using known techniques, offers a challenge to detector technology. But several general-purpose detectors taking full advantage of the SSC's physics potential are expected to meet this challenge.

The capability to increase the luminosity after some years of operation, until it eventually reaches more than 10^{34} cm^{-2} sec^{-1}, will greatly extend the physics reach of the SSC. For many processes, an upgrade from 10^{33} to 10^{34} cm^{-2} sec^{-1} will increase the mass reach for discovering new particles by about 50 percent, in addition to providing higher event rates for known processes. An example of the tradeoff between energy and luminosity, on one hand, and the enhanced discovery potential from increased luminosity, on the other, is given in Figure 3.1.1. The possibility of increasing the luminosity is discussed in more detail in Section 5.2.3.

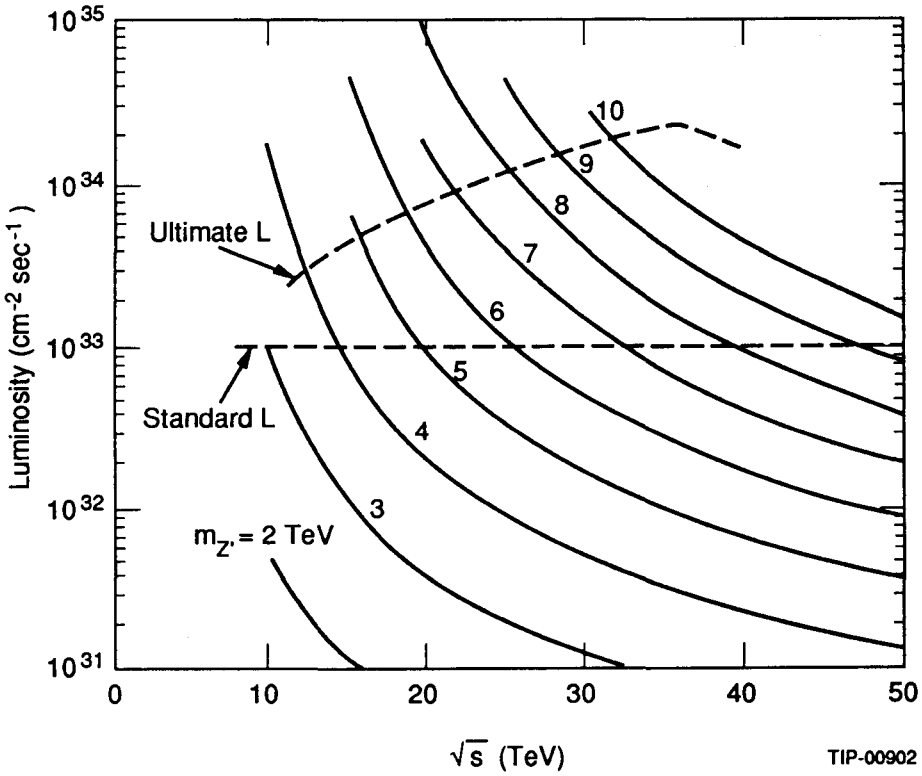

Figure 3.1.1 Luminosity required to produce 100 new Z bosons (Z′) in one year, with standard model couplings, as a function of the center-of-mass energy of proton-proton collisions. Results are shown for mass of the new Z boson in the range from 2 to 10 TeV.

3.1.6 The SSC Laboratory Today

About six hundred Laboratory staff members, visitors, and consultants are now working at the SSC Laboratory offices in south Dallas, a 20-minute drive from the site. The SSC Laboratory is organized in divisions, as shown in Figure 3.1.2. The Project Manager and the Technical Director manage the technical and conventional construction of all accelerator and magnet systems and conventional support facilities. The Physics Research Division defines requirements for experimental support facilities, coordinates the research program, and manages some aspects of general Laboratory support, such as computing. Other divisions provide general administrative and technical support.

The involvement of industrial partners in the operation and management of the Laboratory is unique in high-energy physics. In addition to the work of EG&G and Sverdrup Corporation, assistance with systems engineering is provided by Lockheed Corporation. In March 1990, the consortium of Parsons-Brinckerhoff/Morrison-Knudsen was chosen as the architecture-engineering/construction management firm to carry out the detailed design and construction of conventional facilities in collaboration with Laboratory staff. Industrial contractors will be chosen shortly to participate in the design, development, and production of the superconducting magnets for the SSC.

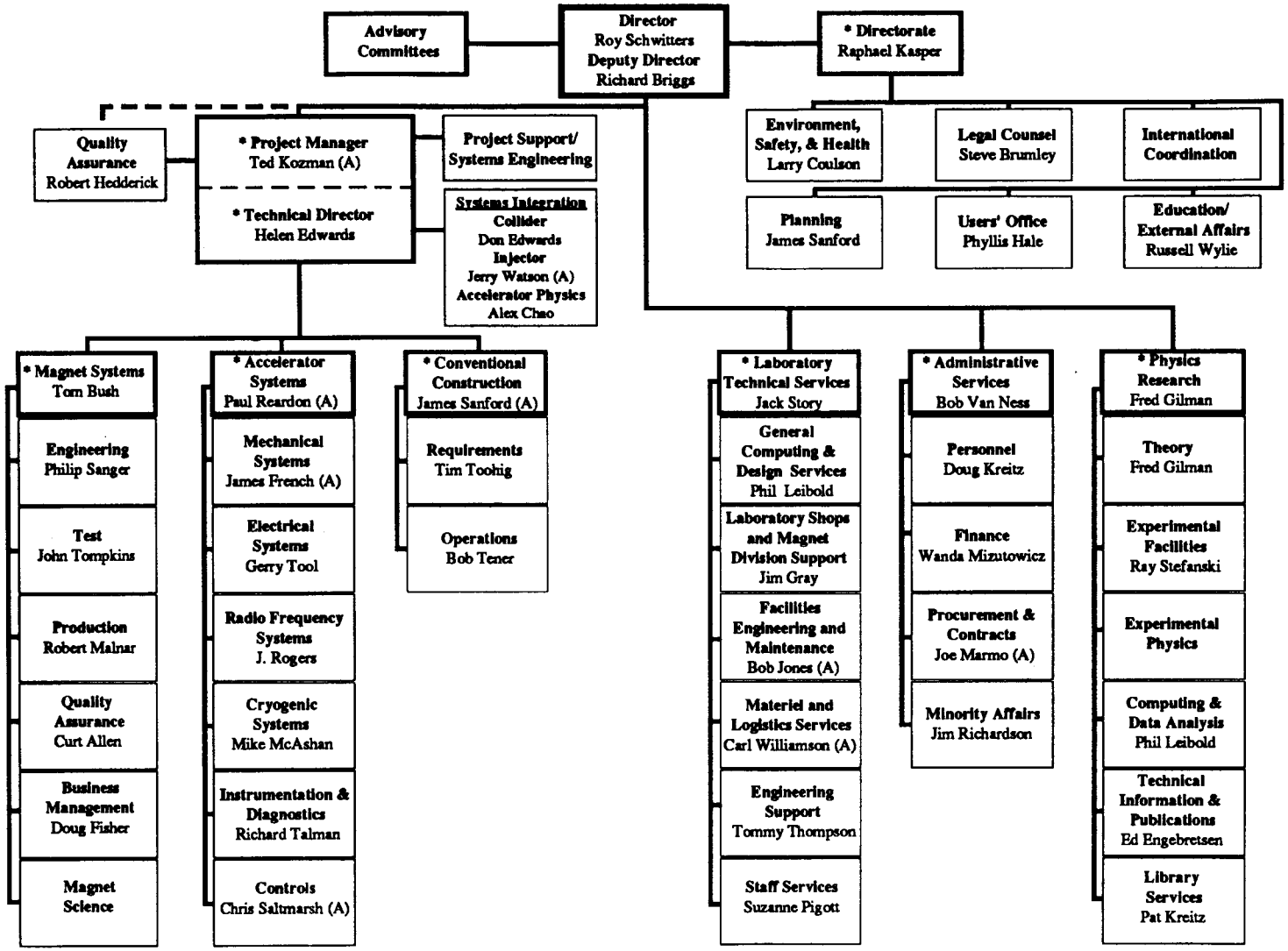

** Laboratory Associate Director*
(A) = Acting

July 23, 1990
SSCL - TIP-00776a

Figure 3.1.2 Organization of the SSC Laboratory.

3.2 Description of the Site and Collider Tunnel

The SSC will be built in Ellis County, Texas, about an hour's drive south of Dallas–Fort Worth in a gently rolling landscape (see Figure 3.2.1.). The site has geological characteristics that are well suited to tunnel boring. The state's proposal for the Ellis County site offered a possible orientation of the collider ring, based on the description of the SSC in the Invitation for Site Proposals. The final position of the collider ring was determined after taking into account a detailed revised design of the collider lattice, the location of the injector complex and experimental halls, and an increased understanding of the underground geology and important surface features of the site. The SSC footprint—a detailed description of the orientation of the injector, collider ring, experimental areas, and surface buildings—is shown in Figure 3.2.2. The land shown within the dotted lines will be acquired by the state of Texas under stratified fee; that is, the right to bore and instrument the collider tunnel will be obtained but surface rights will not. The land shown in the region enclosed by solid lines will be acquired under fee simple, comprising both surface and underground rights. The SSC Laboratory description of the footprint was presented to the Department of Energy in December 1989, and the Department released the footprint description to the state in March 1990.

The relation of the collider tunnel to the geology and topography of the site is shown in Figure 3.2.3. The collider ring consists of four main elements: the north arc, the south arc, the west complex, and the east complex. The arcs are subdivided into 5.4-mile-long sectors. Each sector will have a service area (E) at its center and an auxiliary service area (F) at its end; each sector will use about 50 acres at the surface above the tunnel. The E service areas will support cryogenics in the tunnel, magnet power supplies, electrical power and control systems, personnel and equipment access, and various other utilities. At half of the E areas, a 55-foot-diameter shaft will be dug to permit insertion of superconducting magnets in the tunnel. The F areas will provide support for tunnel ventilation, electrical power and control, and tunnel drainage. A 15-foot-diameter shaft will be located at each F area.

The collider ring tunnel will be excavated primarily by tunnel-boring machines. The finished internal diameter of the tunnel will be about 12 feet; the width at floor level will be about 10 feet. At many locations around the ring there will be alcoves and niches for cryogenic and electrical apparatus. A view of a composite cross section of the tunnel is shown in Figure 3.2.4.

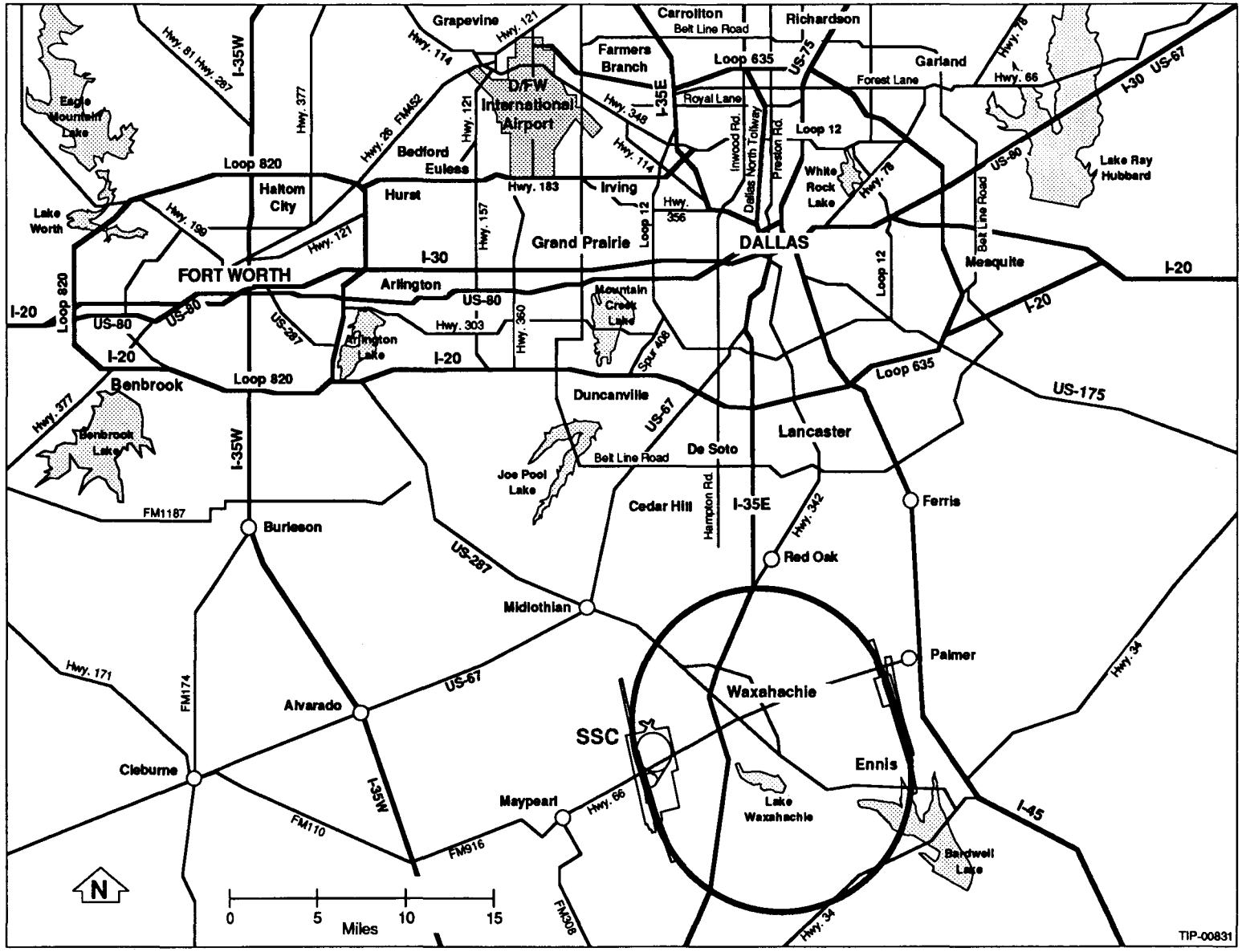

Figure 3.2.1 Location of the SSC site.

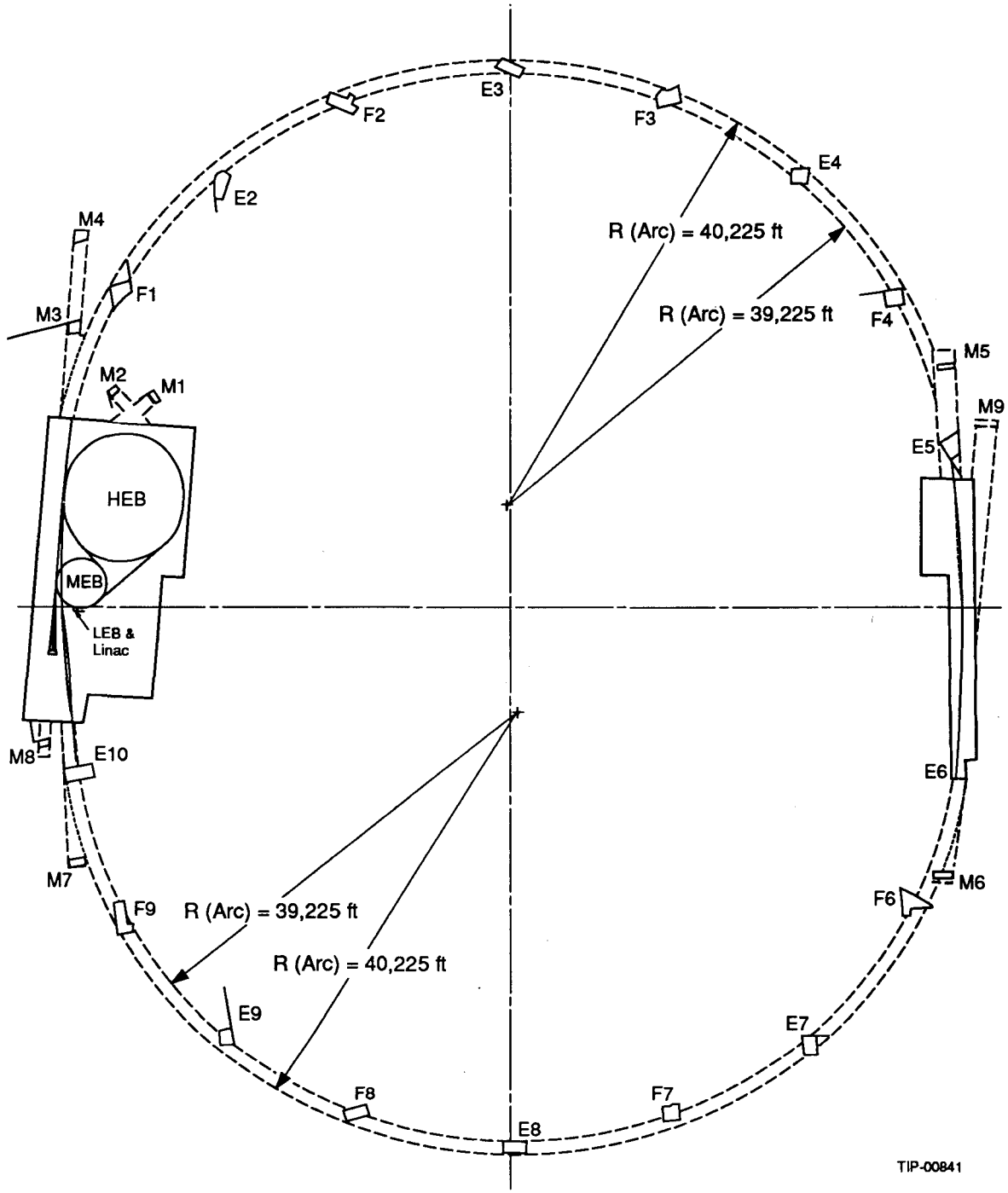

Figure 3.2.2 The SSC footprint.

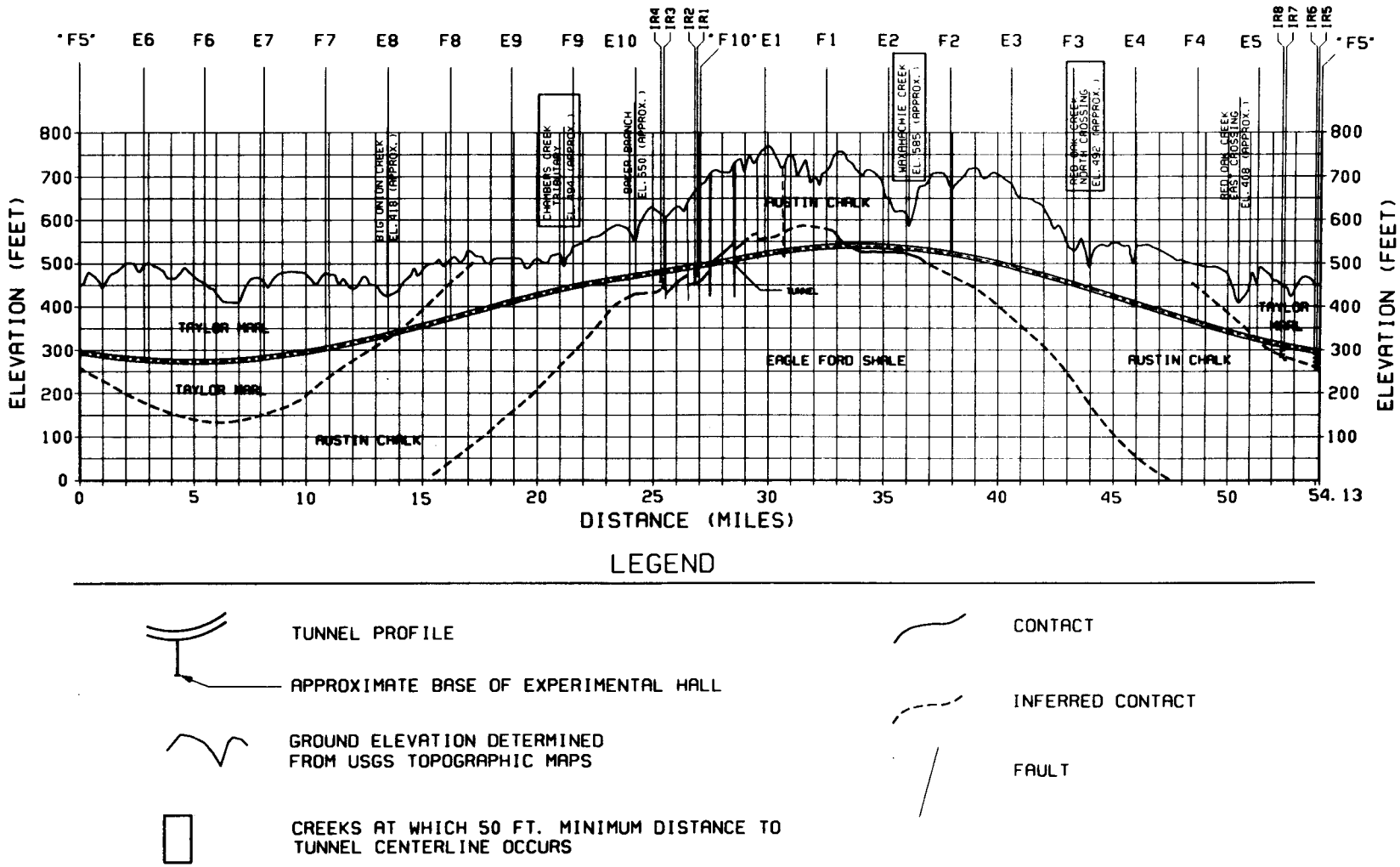

Figure 3.2.3 Schematic relationship of the collider tunnel to the geology and topography of the site.

3.3 Environmental Impact

The SSC Laboratory is strongly committed to preserving and enhancing the environment at the SSC site. The impacts of construction on the environment will be monitored and mitigated as necessary during construction. In September 1989, preparation began of an environmental impact statement (EIS) to supplement the EIS of December 1988, written before the final site selection. It is expected that the supplemental EIS will be completed in the last quarter of 1990.

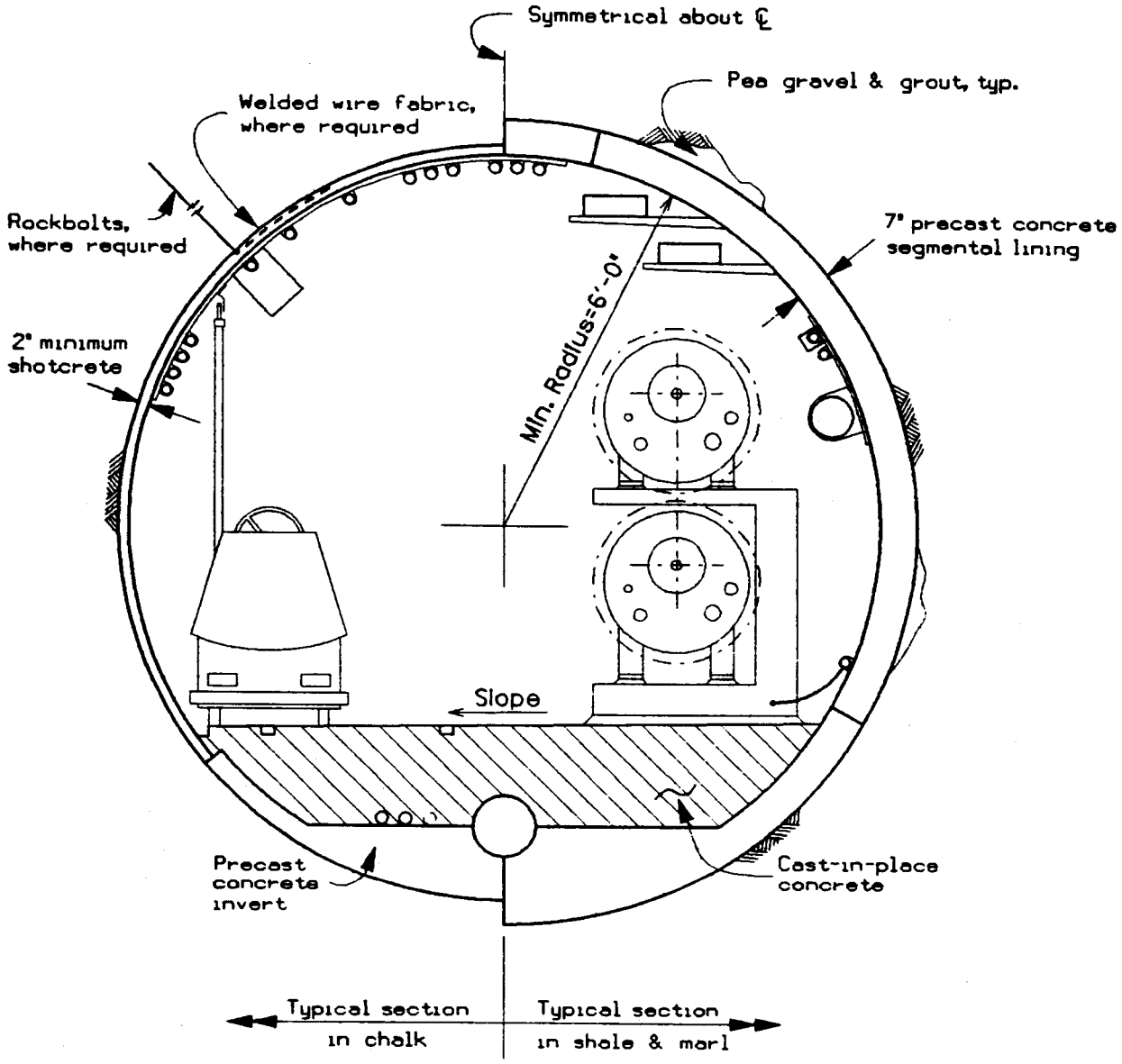

Figure 3.2.4 Cross section of the collider tunnel.

4. The SSC Research Complex

4.1 A Reliable, Flexible Design

The SSC Laboratory is committed to providing an accelerator that will reliably deliver both colliding beams and external beams (for test and calibration of apparatus) soon after the initial commissioning of the accelerators. The Laboratory is also dedicated to providing an opportunity for researchers from around the world to carry out experiments addressing all aspects of the physics potential at the SSC as early as possible. The SSC conceptual design is a timely, cost-effective approach to providing an accelerator and experimental complex that will meet these goals, while maintaining the flexibility to respond to new directions in particle physics.

4.2 The Accelerator Complex

The description of the accelerator complex presented here cannot summarize in any detail the wealth of material available on the design of the accelerators and their components. The SCDR provides a detailed description of the accelerator systems (Chapter 4) and the associated civil construction (Chapter 6). This summary provides only an overview of accelerator parameters and briefly discusses the accelerator components—primarily the collider superconducting dipoles—and the choices of key parameters.

4.2.1 Overview of the Accelerators

Five cascaded accelerators will ultimately provide the collisions of two 20-TeV proton beams. The first four accelerators will accelerate proton beams and inject them into the collider at an energy of 2 TeV. A schematic layout of the injector complex is shown in Figure 4.2.1. The collider itself consists of two rings of superconducting magnets, one 0.8 m above the other, that intersect at four points around the ring to provide collisions for experiments. Eight arc sectors and two cluster regions make up the collider. In one part of a cluster, the beams are brought into collision in two interaction regions; the other part is used to inject or remove the beam and to provide space for radio-frequency cavities (for acceleration of the beam in the collider rings). Interaction regions are located on one half of a diamond-shaped bypass; the other half will be available for a future upgrade (Section 5.2.1). Key design parameters of the collider are summarized in Table 4.2.1.

The precise layout of the injector complex is determined not only by physics considerations but also by the site. The high-energy booster (HEB) is at approximately the same depth as the collider ring; there is one utility straight section in the high-energy booster for transferring beam into both collider rings. The significant surface elevation change over the area of the high-energy booster means that the high-energy booster could not reasonably be located near the surface. However, the smaller linac, low-energy booster (LEB), and

medium-energy booster (MEB) can all be accommodated near the surface. Beams will be transferred down from the medium-energy booster to the high-energy booster through two transfer lines. The high-energy booster and the medium-energy booster are tangent to a line through the test beam area, so beams from both the high-energy booster and the medium-energy booster could potentially be extracted to produce secondary beams. In the initial configuration, only beams derived from the medium-energy booster will be available; beams from the high-energy booster could be made available in a future upgrade. Some parameters of the collider and of the injector accelerators are summarized in Table 4.2.2.

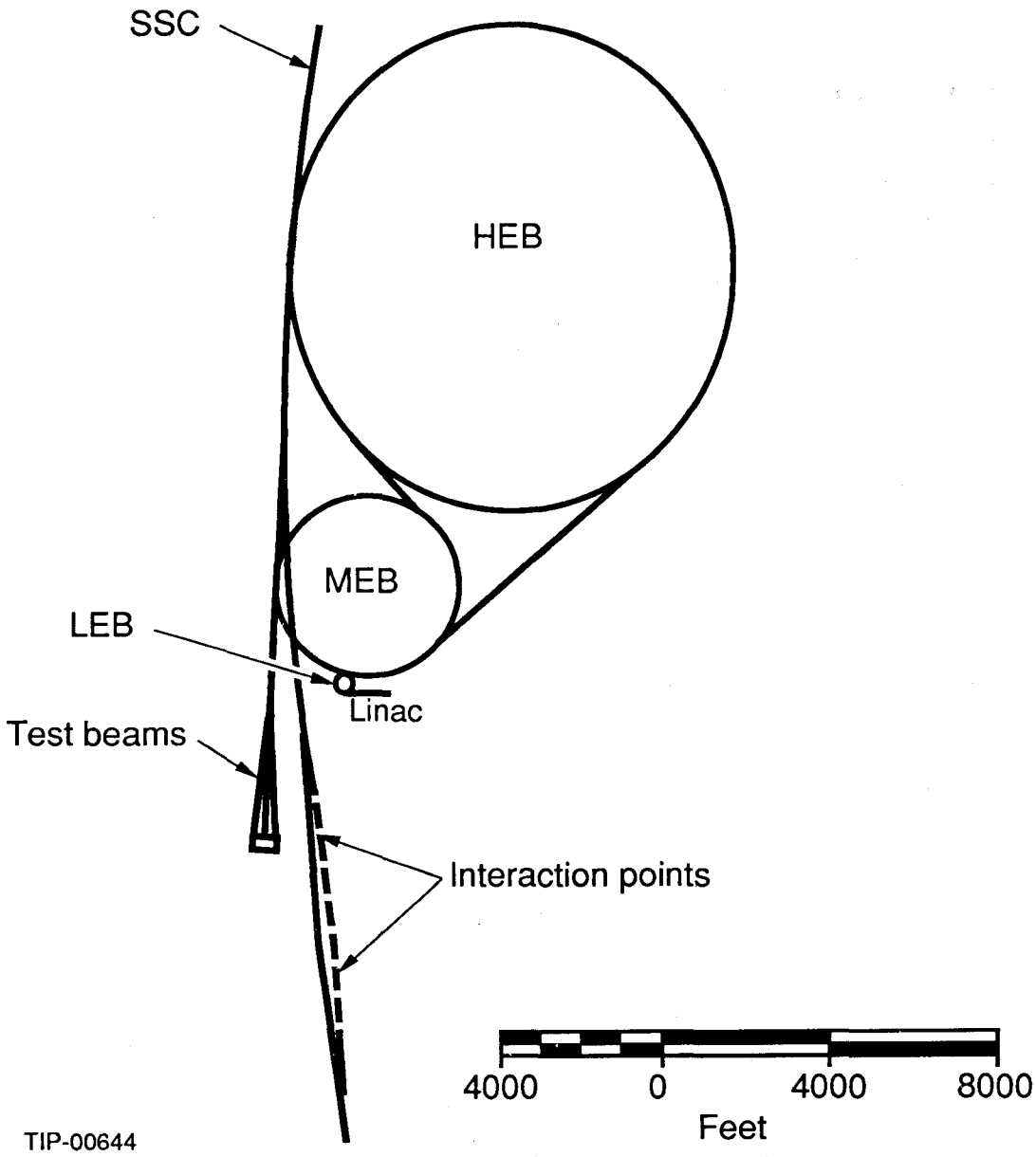

Figure 4.2.1 Schematic layout of the injector complex, a portion of the collider ring and the test beam area. The dashed line indicates a future beam bypass.

Table 4.2.1
Key parameters of the collider

Energy: injection, collision (TeV)	2	20
Magnetic radius (ρ) (m)	10187.1896	
Magnetic field (B_0) (T)	6.59994	
Rigidity ($B\rho$) (T-m)	66712.8	
Gradient (G) (T/m)	205.5892	
Circumference (484 cell lengths) (km)	87.12	
Arc length, cluster length (km)	35.28	8.28
Half-cell length, arc sector length (m)	90	4320
Long straight section length, bypass length (m)	1350	4770
Drift lengths at IP: low-β, medium-β IRs (m)	±20	±120
Drift lengths in utility straight: center, ends (m)	500	161
IP-IP distance: inner, outer (m)	2160	2520
IP-IP bending angle (mrad)	40	
Minimum IP-to-muon-beam clearance (m)	34	
Vertical beamline separation (m)	0.80	
Cell phase advance (deg)	90	
Betatron tune: outer, inner bypass branch	123.28	123.78
Phase advance between IPs	$4.25 \times 2\pi$	$3.75 \times 2\pi$
Chromaticity: collision, injection optics	–250	–173
Transition γ	104.6 (inner)	105.0 (outer)
Momentum compaction ($1/\gamma_t^2$)	0.000091	
Crossing angle (μrad)	<150	
Bunch spacing (m)	5	
rf wavelength (λ_{rf}) (m)	0.8333	
Lengths of cell dipoles, quadrupole (effective) (m)	15.2 and 12.6	5.2
Bend radius, average arc radius (km)	10.187	12.032
Bend angle per arc, per cluster (deg)	168	12
Maximum number of IRs: simultaneous, total	5	9
Cells per arc, cluster length in equivalent cells	196	46
Number of dipoles per cell	10	
β_{max}, β_{min} in arc (m)	305	53
η_{max}, η_{min} in arc (m)	1.82	0.8
β^* in low-β IR: injection, collision (m)	8	0.5
β^* in medium-β IR: injection, collision (m)	60	10
β_{max} in low-β, medium-β IRs (collision) (m)	7990	2657
β_{center}, β_{max} in utility straight (m)	300	970

Table 4.2.2
Parameters of the collider ring and the injector complex accelerators

	LEB	MEB	HEB	Collider
Revolution time (μs)	1.80	13.2	36.3	290.4
Extraction momentum (TeV/c)	0.012	0.2	2.0	20.0
Injection momentum (TeV/c)	0.0012	0.012	0.2	2.0
Ratio of circumference to previous ring	—	7-1/3	2-3/4	8
Half ring cog time for ±5 mm (μs)	—	216	6400	—
Transition γ	14.5	15.94	29.19	104.6
Range of synchrotron frequencies (Hz)	48–21,000	77–450	3–54	4.3–11
Energy gain per turn (max) (keV)	609	2680	1815	5808
Typical synchronous phase (deg)	60	138	150	160
$(1 - v_{out}/c)$	3.0×10^{-3}	1.1×10^{-5}	1.1×10^{-7}	1.1×10^{-9}
$(1 - v_{in}/c)$	0.208	3.0×10^{-3}	1.1×10^{-5}	1.1×10^{-7}
Half-cell length (m)	5.0	22.5	38.9	90
Min. typical bunch σ_t (ns)	0.36	0.25	0.26	0.16
Max. typical bunch σ_t (ns)	3.3	0.87	0.95	0.20
Min. typical bunch $\sigma p/p$ ($\times 10^{-3}$)	0.20	0.053	0.019	0.057
Max. typical bunch $\sigma p/p$ ($\times 10^{-3}$)	0.88	$\lesssim$0.50	0.082	0.120
Space charge $\Delta\nu_{max}$ for collider op.	0.34	$\lesssim$0.15	0.0017	0.0010
Min. typical impedance threshold for collider operation (Ω)	5.2	$\lesssim$4.7	2.6	1.7

4.2.2 Design Parameters

The next two subsections describe the design of the collider and the injector systems in more detail. The technical components of these accelerators are described in Section 4.2.3.

4.2.2.1 The Collider

Both collider rings have two nearly circular arcs in the north and south regions of the ring and two clusters of long straight sections in the east and west regions. Two proton beams, one in each ring of superconducting magnets, will circulate in opposite directions. As viewed from above, the beams in the top ring will travel counterclockwise.

Each cluster contains one utility straight section and one diamond-shaped bypass, one leg of which will be operational in the initial configuration of the collider. The utility straight section in the west cluster will be used for injection from the high-energy booster, for extraction of spent beam into beam dumps, for beam scraping, and for rf systems. The east utility straight section, which will not be used in the initial configuration, could be converted later into an interaction region with horizontal rather than vertical crossing of the beams.

In plan view, the collider ring has two superperiods, one of which is shown in Figure 4.2.2. From top to bottom, the figure shows the superperiod starting in a clockwise direction from the beginning of a cluster, then moving through that cluster and the succeeding arc.

The north and south arcs are composed of periodic FODO cells whose main functions are to bend the beam around the ring and to keep it focused transversely. The quadrupoles in the arcs are 90 meters apart and alternate in the sign of their gradient. The arc structure

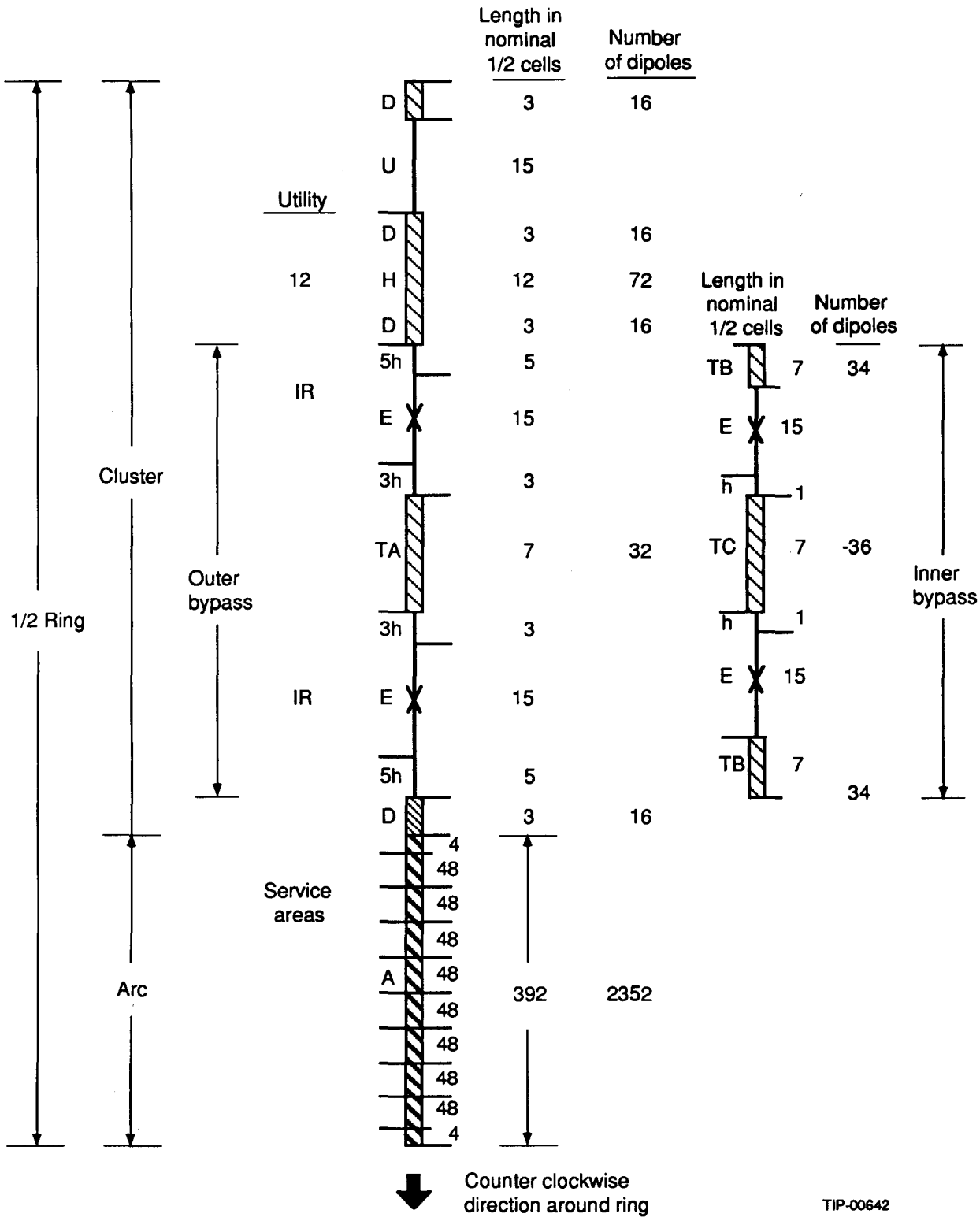

Figure 4.2.2 Schematic arrangement of the lattice components in a superperiod. D is a dispersion suppressor section, U a utility straight section, H a bending region of 12 half-cells, TA a transition region, and E the interaction region sandwiched between five half-cells without bends, h, on one side and three on the other. The arc, A, consists of 392 half-cells.

repeats every 180 m (that is, every cell), and each cell consists of two half-cells that differ only by the sign of the quadrupole gradient. Five dipoles are located in each half-cell (see Figure 4.2.3). In addition, there is a spool piece (SPE) at one end of the cell for correctors and various attachments and a smaller spool piece (SPC) for mid-cell correctors.

The other major components of the collider lattice are the dispersion suppressors, the transition regions, the utility straight sections, and the interaction regions. A dispersion suppressor is a lattice component that forms a bridge between a section of the lattice that has dispersion typical of the arc cells and another section that has zero dispersion. It consists of two cells, each three-quarters as long as a normal cell and with two-thirds the total bend. A transition region is the bending section of the bypass. The utility straight sections serve as points of injection, extraction, and scraping (see Figure 4.2.4). The interaction regions are described in Section 4.3.

The linked issues of the energy at which beams are injected into the collider and the diameter of the magnet aperture have been intensively investigated. The present design has an injection energy of 2 TeV and a magnet aperture of 50 mm. The rationale for these decisions is discussed in detail in the SCDR, in references in the SCDR, and in other documents.[5] Both a Machine Advisory Committee[6] and a HEPAP subpanel[4] have reviewed and reaffirmed these values as necessary to ensure timely operation of the collider.

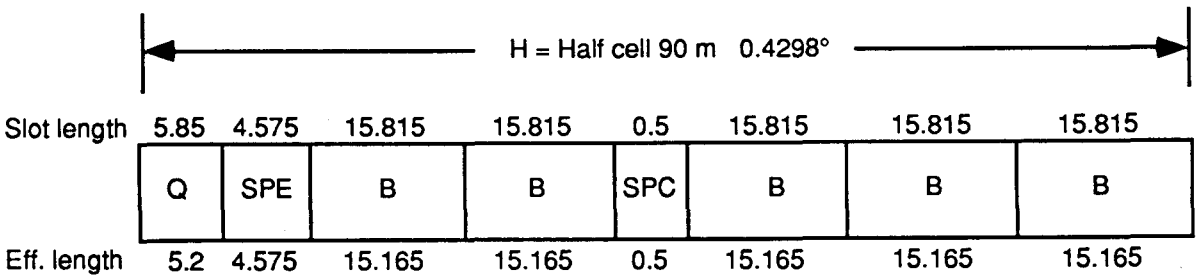

Figure 4.2.3 Location of the magnets in a typical arc half-cell.

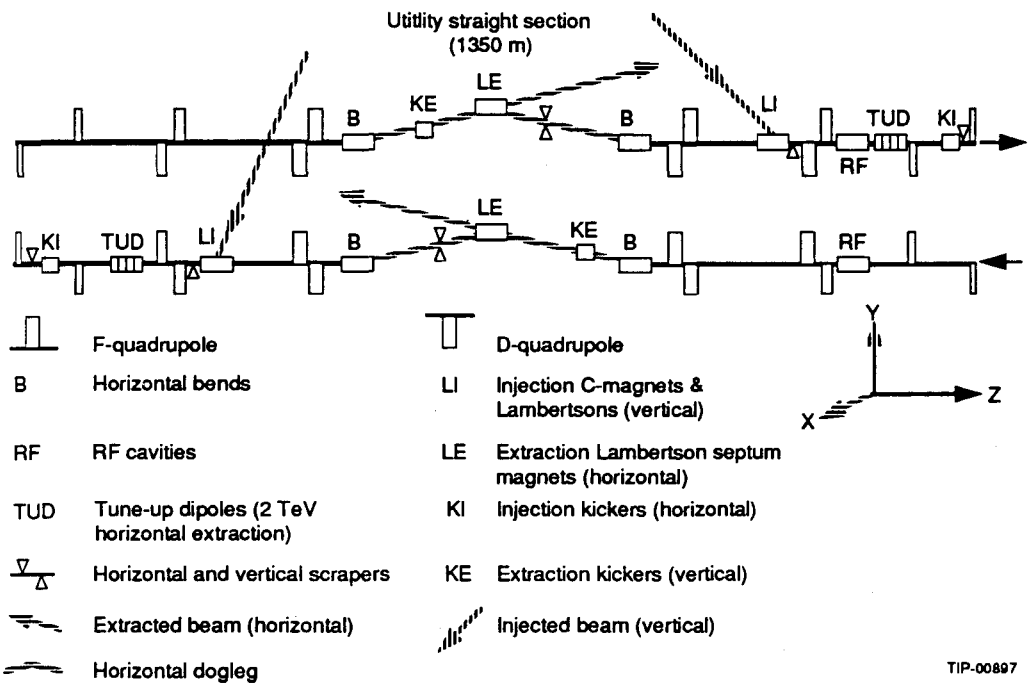

Figure 4.2.4 Schematic view of a utility straight section.

4.2.2.2 The Injector Systems

This section summarizes the properties of the injection system, the linac, the low-energy booster, the medium-energy booster, and the high-energy booster. An expanded view of the injector complex is given in Figure 4.2.5.

The injector complex must satisfy a number of demanding requirements. It must operate in two modes: to inject 2-TeV protons into the collider rings when necessary (about once a day) and to continually produce extracted beams for the test beam facility. The injector parameters must also accommodate a future increase of peak luminosity above the design value of 10^{33} cm^{-2} sec^{-1}.

The high-energy booster is a 2-TeV superconducting synchrotron. The dipoles in the high-energy booster will provide a field of 6.4 T at a temperature of 4.35 K. To use space most efficiently, the high-energy booster will be capable of bipolar operation for collider injection. The aperture and field qualities of the high-energy booster magnets are being evaluated to determine the feasibility of resonant slow extraction to provide an external 2-TeV beam, which might be desirable for a future upgrade of the test beam facility. The basic design of the high-energy booster consists of two nearly semi-circular arcs connected by two long straight sections. One straight section will be used for fast extraction and injection into the collider rings and for extraction into the test beam area. The other straight section will contain electrostatic septa to allow extraction into the test beam line on the other side of the high-energy booster. The operating cycles of the high-energy booster are described in Chapter 5. The high-energy booster parameters are summarized in Table 4.2.3.

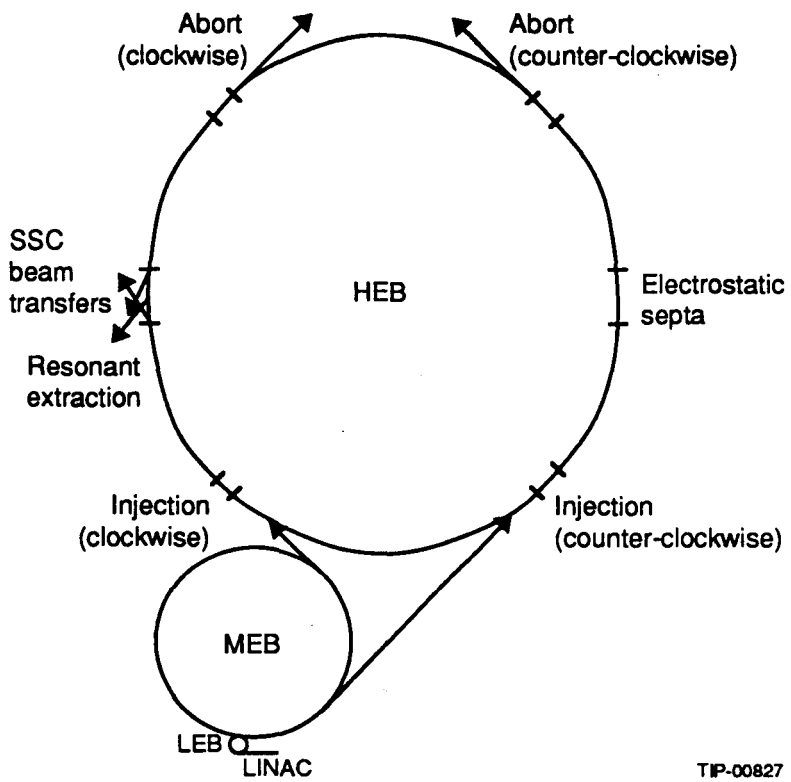

Figure 4.2.5 Schematic view of the injector complex.

Table 4.2.3
Parameters of the high-energy booster

Momentum: injection, extraction (GeV/c)	200	2000
Circumference (km)		10.890
Tunnel depth (m)		~46
Operational mode		bipolar
Structure		
Lattice type		FODO
No. of superperiods		2
No. of arcs		6
No. of long straight sections (LSS)		2
No. of short straight sections (SSS)		4
Straight-section functions and component locations		
Injection, CW (vertical)		SW SSS
Injection, CCW (vertical)		SE SSS
Abort, CW (vertical)		NW SSS
Abort, CCW (vertical)		NE SSS
Extraction to collider, CW and CCW (vertical)		W LSS
Test-beam extraction, CCW (vertical)		W LSS
Resonant-extraction electrostatic septa (horizontal)		E LSS
Radio-frequency acceleration cavities		W LSS
Magnet type		SC
Dipole field, quadrupole gradient, 2 TeV	6.40 T	206 T/m
Dipole coil i.d. (mm)		50
Bunch spacing (m)		5.0
Accelerating frequency (MHz)		60.0
Harmonic no.		2178
Rf voltage, peak (MV)		2.6
Synchronous phase (deg)		30
Protons per bunch: collider, test beam	1×10^{10}	5×10^{10}
rms norm. trans. emittance: collider, test beam (mm-mrad)	$0.8\ \pi$	$4\ \pi$
rms long. emittance: 200 GeV, 2 TeV (eV-s)	$0.0040\ \pi$	$0.035\ \pi$
Cycle time: collider injection, test beams (min)	2	3

The medium-energy booster is an accelerator using conventional magnets designed to deliver 200-GeV proton beams to the high-energy booster and to the test beam area. Beams will be extracted and injected into the high-energy booster both clockwise and counter-clockwise. The design injection momentum into the high-energy booster is 12 GeV/*c*. The parameters of the medium-energy booster are summarized in Table 4.2.4.

The low-energy booster is a conventional accelerator designed to accelerate proton beams from the injection kinetic energy of 600 MeV up to an extraction momentum of 12 GeV/*c*. The parameters of the low-energy booster are given in Table 4.2.5.

Table 4.2.4
Parameters of the medium-energy booster

Maximum momentum	200 GeV/c
Injection momentum, possible	12, 9 GeV/c
Circumference	3960 m
Tunes	16.6
Cell phase advance	59.8 deg
Transition gamma	15.94
Natural chromaticity	–18.1
Operation	monopolar
Dipole field at 200 GeV/c	1.698 T
Dipole effective length	7.575 m
Dipole slot length	7.9 m
Bend radius	392.8 m
Horizontal good field aperture	90.0 mm
Half-cell length	19.8 m
Dipoles per half-cell	2
Total number of dipoles	328
Total number of cells	100
Quadrupole gradient at 200 GeV/c	17.4 T/m
Quadrupole effective length	2.0 m
Quadrupole slot length	2.3 m
Number of quadrupoles	200
Number of sextupoles	216
Number of sextupole families	3
Int. sextupole strength (Bdl)	8 kG-in. at 1 in.
Maximum amplitude function	67 m
Minimum amplitude function	24 m
Maximum dispersion function	3.8 m
Minimum dispersion function	1.0 m
Number of straight sections	8
Bunch intensity (collider fill)	1×10^{10}
Normalized emittance (rms/collider fill)	1 π mm-mrad
Bunch intensity (slow spill)	5×10^{10}
Normalized emittance (rms, slow spill)	4 π mm-mrad
Space charge tune shift (injection)	0.07
rf wavelength	5.0 m
rf at 12 GeV/*c*, at 9 GeV/c	59.776, 59.635 MHz
rf at extraction	59.958 MHz
rf peak voltage	4.0 MV
Cycle time (HEB transfer)	3.0 sec
Cycle time (test beam slow spill)	4.0 sec
Depth	near surface

Table 4.2.5
Parameters of the low-energy booster

Injection momentum, kinetic energy	1.219 GeV/c, 600 MeV
Extraction momentum	12 GeV/c
Circumference	540 m
Harmonic number	108
Bunch spacing	5 m
Operation	unipolar
Protons per bunch (collider operation)	10^{10}
Protons per bunch (fixed target operation)	5×10^{10}
Transverse emittance (collider operation) (normalized, rms)	0.6π mm-mrad
Transverse emittance (fixed-target operation) (normalized, rms)	4π mm-mrad
Longitudinal emittance	$2\pi \times 10^{-3}$ eV-s, rms
Lattice type	FODO
Half-cell length	5 m
Phase advance per cell	112 deg
Superperiodicity	6
Betatron tunes (H/V)	16.85/16.75
Transition gamma	14.5
Chromaticities (H/V)	–25.15/–25.16
β_{max}/β_{min}	19.4/1.85 m
η_{max}/η_{min}	1.03/–0.09 m
Number of dipoles	84
Dipole length (effective)	2.43 m
Dipole field (max)	1.23 T
Full dipole aperture (H/V)	8.0/5.72 cm
Number of quadrupoles (F + D)	108
Quadrupole length (effective)	0.85 m
Quadrupole gradient (B', max)	16.5 T/m
Quadrupole pole tip radius	4 cm
Number of F-sextupoles	42
Number of D-sextupoles	48
Sextupole length (effective)	0.2 m
Sextupole pole tip radius	5 cm
F-sextupole pole tip field (Bl at 5 cm)	0.0375 T-m
D-sextupole pole tip field (Bl at 5 cm)	0.0755 T-m
rf at injection	47.513 MHz (52.465 at 1 GeV kinetic energy)
rf at extraction	59.776 MHz (59.635 at 9 GeV/c momentum)
rf peak voltage (total)	700 kV
Number of rf cavities	8
Cavity length	1 m

The linac consists of an H^- ion source, followed by a radio-frequency quadrupole accelerator, a drift-tube linac, and a coupled-cell linac. Like the other elements of the injector complex, the linac will also operate in two modes: one for filling the collider ring and one for test beam operation. The parameters of the linac design are summarized in Table 4.2.6.

The accelerators in the injector complex require accelerator tunnels and surface buildings to house utilities and controls. These conventional construction aspects of the design are described in detail in Chapter 6 of the SCDR.

Table 4.2.6
Parameters of the linac

H^- Source	
Type	Magnetron
Voltage	35 kV
Design current	30 mA
Length (with non-neutralized LEB)	1 m
RFQ (radio frequency quadrupole)	
Type	4-vane
Frequency	428 MHz
Output energy	2.5 MeV
Design current	26 mA
Total power	0.4 MW, 1 Klystron
Length	2.2 m
DTL (drift-tube linac)	
Type	ramped and constant gradient, perm. magnet
Frequency	428 MHz
Output energy	100 MeV
Design current	25 mA
Total power	18 MW, 6 Klystrons
Length	35 m
CCL (coupled-cell linac)	
Type	Side-coupled
Frequency	1284 MHz
Output energy	600 MeV
Design current	25 mA
Pulse length	$< 35\ \mu s$
Repetition rate	10 Hz
Transverse emittances (n, rms)	$0.25\ \pi$ mm-mrad
Longitudinal emittance (rms)	0.07×10^{-5} eV-s
Total power	150 MW, 10 Klystrons
Length	110 m

4.2.3 Technical Components

Construction and operation of SSC accelerators requires a large number of reliable technical components. This summary focuses on the superconducting magnets, primarily the dipoles, for the collider; on the cryogenic systems; and on beam instrumentation and controls. Detailed descriptions of all components are given in Chapter 4 of the SCDR.

4.2.3.1 Superconducting Magnets for the Collider

The collider's superconducting magnet system bends and focuses the proton beams in the storage rings and guides the beams into collision at the interaction points. The critical elements in this system are the thousands of superconducting collider dipole magnets that must operate with very high reliability during the lifetime of the SSC collider. All the collider magnets are required to survive over 10^4 accelerator cycles, in which the field varies from that required to bend the path of the protons at the 2 TeV injection energy to that required at the 20 TeV collision energy. In addition, the magnets will be required to withstand about 50 thermal cycles from room temperature to the operating temperature of about 4 K. Finally, the magnetic field must ensure reliable storage of the beam at injection, during ramping to 20 TeV, and for day-long stretches at the collision energy.

The magnetic field is created by currents in both inner and outer magnet coil layers. Superconducting cable is carefully positioned in a cosine-theta geometry to provide the dipole field while keeping other components of the field within tolerance.

A schematic view of a collider dipole is shown in Figure 4.2.6. The major components are the coils of NbTi superconductor in a copper matrix, the collar that holds the coils rigidly in place under the large magnetic forces, and the cold-iron yoke. This "cold mass" is mounted in a cryostat that uses a folded support system to keep heat leaks to a minimum and that fully supports the magnet during shipping and installation (see Figure 4.2.7).

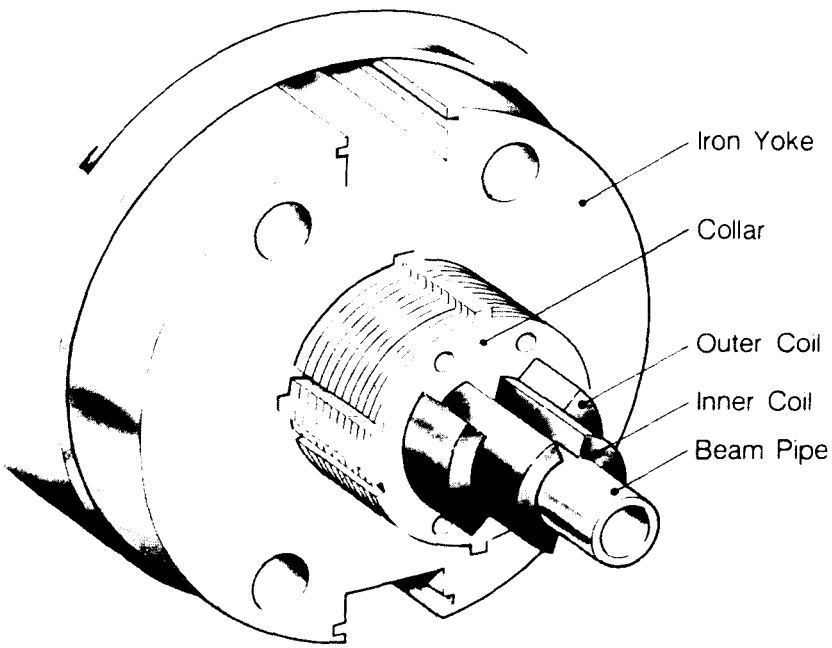

Figure 4.2.6 Schematic layout of the major components of a collider dipole cold mass.

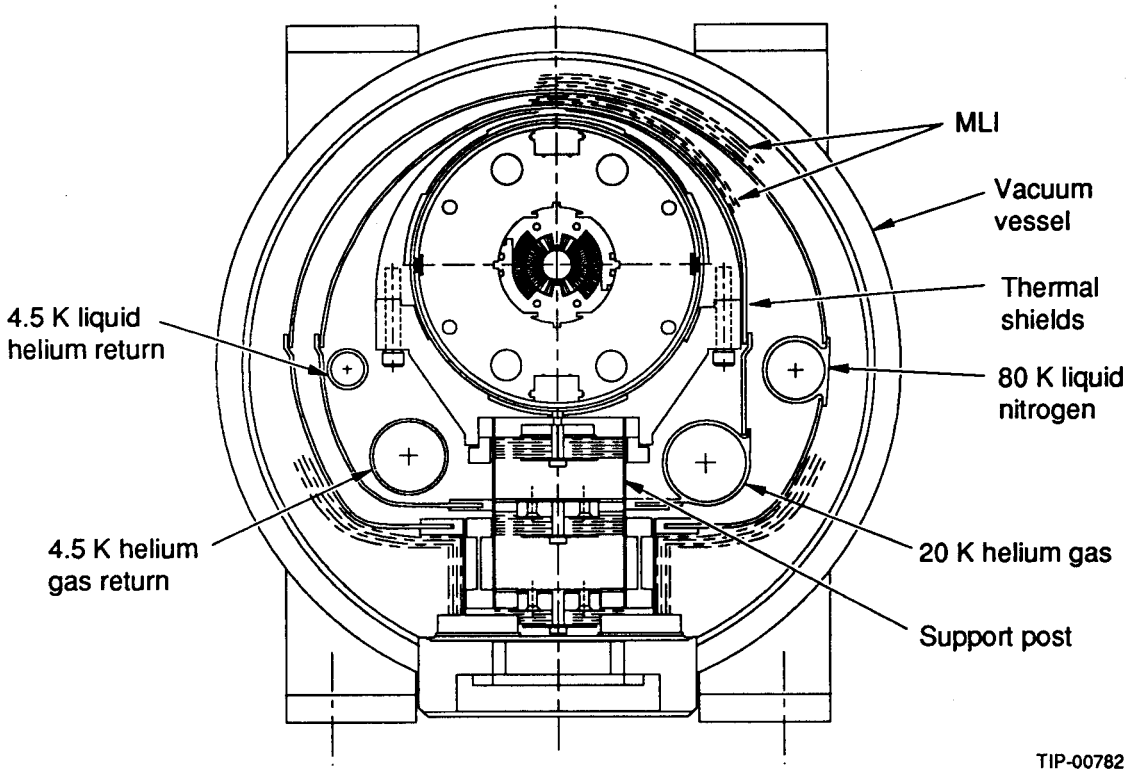

Figure 4.2.7 Cross section of a collider dipole magnet in the cryostat.

Dipole magnets of two lengths—about 15 m and 13 m—are required for the collider lattice. The operating field at 20 TeV is about 6.6 T at a temperature of 4.35 K. Although a 17-m magnet with an aperture of 40 mm was envisioned in the 1986 Conceptual Design Report, in the recent formulation of the collider lattice design it was decided to use shorter dipole magnets of two lengths and to increase the aperture of the magnet to 50 mm. The larger the magnet bore, the higher the cost, but the better the field quality. It is believed that the current design of the collider dipole will provide the requisite quality at minimum cost.

The standard expression for the multipole coefficient representation of the magnetic field is given by

$$B_y + iB_x = B_0 \sum_{n=0}^{\infty} (b_n + ia_n)(x + iy)^n ,$$

where the coefficients a_n and b_n are given in units of 10^{-4} cm^{-n}. A good magnet has multipole coefficients within an acceptable range of values, determined by beam stability requirements. The multipole values depend in detail upon the placement of the conductor, the arrangement of the iron, and the state of the superconductor magnetization. The last variable introduces a time dependence of the multipole content of the field, so the specifications of allowed multipole content depend on assumptions about the magnetic cycle of a magnet. Two tolerances are used, one arising from random errors (in conductor placement, for example) and the other from systematic shifts. The tolerances assumed for the collider dipoles are given in Table 4.2.7.

Table 4.2.7

Tolerances for the collider dipole multipoles: (a) rms tolerances that apply at all field values from injection to collision and (b) allowed systematic tolerances on the absolute value of the multipole value at injection and at collision.

(a) Specifications for rms distribution of collider dipole multipoles

Multipole	rms Width (σ spec)
a_1	1.25
b_1	0.50
a_2	0.35
b_2	1.15
a_3	0.32
b_3	0.16
a_4	0.05
b_4	0.22
a_5	0.05
b_5	0.02
a_6	0.01
b_6	0.02
a_7	0.01
b_7	0.01
a_8	0.0075
b_8	0.0075

(b) Specification for the systematic multipole absolute value*

Multipole	Injection	High Field
$\lvert a_1 \rvert$	<0.04	<0.04
$\lvert b_1 \rvert$	<0.04	<0.04
$\lvert a_2 \rvert$	<0.032	<0.032
$\lvert b_2 \rvert$	<2.00[a]	<0.80
$\lvert a_3 \rvert$	<0.026	<0.026
$\lvert b_3 \rvert$	<0.026	>0.026
$\lvert a_4 \rvert$	<0.02	>0.02
$\lvert b_4 \rvert$	<0.08[b]	<0.08
$\lvert a_5 \rvert$	<0.016	<0.016
$\lvert b_5 \rvert$	<0.016	<0.016
$\lvert a_6 \rvert$	<0.013	<0.013
$\lvert b_6 \rvert$	<0.02	<0.013
$\lvert a_7 \rvert$	<0.01	<0.01
$\lvert b_7 \rvert$	<0.01	<0.01
$\lvert a_8 \rvert$	<0.008	<0.008
$\lvert b_8 \rvert$	<0.02	<0.02

[a] Value of systematic b_2 must not change by more than 0.5 units during the 1-hr injection interval.
[b] Value of systematic b_4 must not change by more than 0.04 units during the 1-hr injection interval.
* Systematic multipole error is defined as the average value of the multipole. The average is taken over the entire sample of magnets installed in a collider ring. No magnet shall be accepted that deviates by more than 3σ spec from the average value of any multipole.

The main emphasis of the dipole magnet research-and-development program over the last few years has been the mechanical design and quench behavior of the magnets. The substantial magnetic forces on the conductor can cause microscopic motion of the conductor, giving rise to local heating and thereby quenching a magnet. Magnets have been instrumented to determine the location of quenches and to measure the forces on the collars constraining the coils. The results have been compared with model calculations to obtain a fundamental understanding of the mechanical behavior of the research-and-development magnets. A history of the quench behavior of recent long research-and-development magnets is given in Figure 4.2.8. The lesson to be drawn is that preventing conductor motion is imperative. Achieving that aim requires detailed designs and calculations as well as strict adherence to quality control standards. A number of the early research-and-development magnets exhibited quench behavior well below the theoretical value because of mistakes during assembly.

For a dipole magnet to be acceptable, it must not quench below the operating field during initial testing or after thermal cycling. It must also

- remain useful for at least 25 years,
- withstand 50 thermal cycles, while retaining allowable field qualities,
- withstand 100 quenches, and
- withstand 2×10^4 magnetic cycles.

To determine the ability of the magnets to meet these requirements, accelerated life tests will be performed on prototype collider dipoles in the next two years.

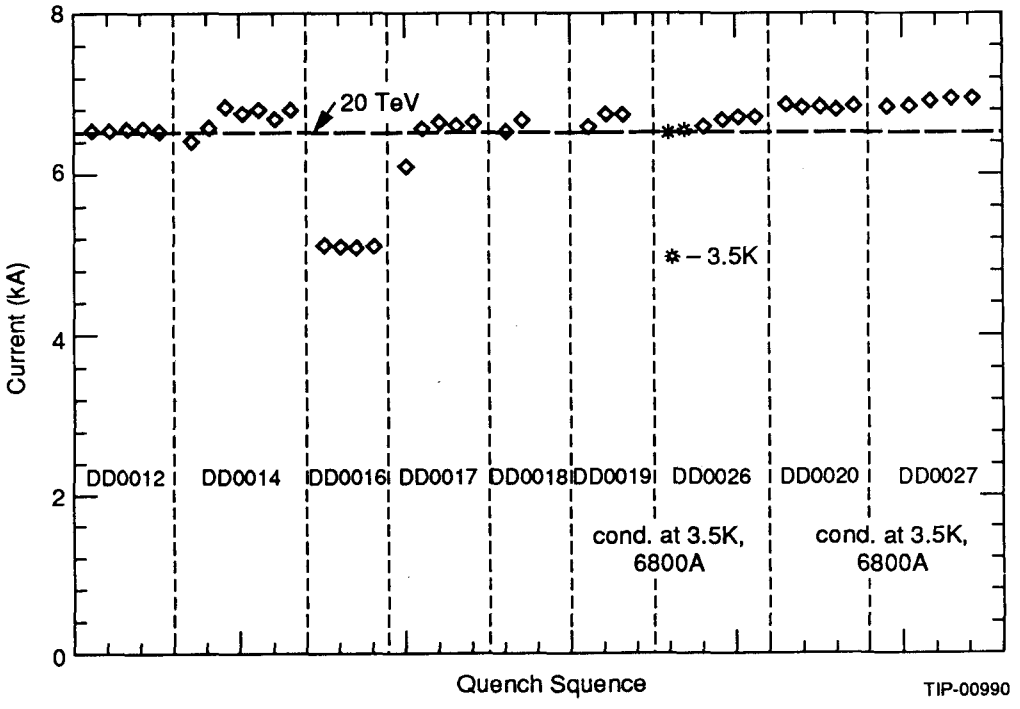

Figure 4.2.8 A composite series of training curves for recent long (17 m) R&D collider dipoles. The current at quench depends in detail upon the operating temperature, which is not given for each point on the curves.

The superconducting wire used in the magnets is the result of years of collaborative research and development between industrial suppliers and the SSC project. There has been substantial improvement in the critical current density capacity, a key parameter. Wire now exists that satisfies the minimum critical current density requirement for both inner and outer coils. In addition to providing a high current density, wire with fine filament sizes must also be provided in order to reduce the effects of persistent currents at low field. The specification for the collider magnets is a filament diameter of 6 μ, although research and development continue to reduce this size for the HEB. (The exact wire requirements depend upon the coil layer in which it will be used; see Table 4.2.8.)

Table 4.2.8
Parameters of NbTi superconducting wire for the SSC magnets

	Inner Layer	Outer Layer
NbTi composition (% Ti)[a]	47.0	47.0
Critical current (A)	339[b]	286[c]
J_c (non-Cu) (A/mm^2)	1730[b]	2540[c]
Copper-to-superconductor ratio	1.5:1	1.8:1
Filament diameter (μm)	6	6
Strand diameter (mm)	0.808	0.648
No. of filaments	8000	4400
Strand twist pitch (per m)	40	40
Copper residual resistance ratio, R_{295}/R_{10}	>70	>70

[a]High-homogeneity material
[b]At 7.0 T, 4.2 K, and a resistivity of 10^{-14} Ω-m
[c]At 5.6 T, 4.2 K, and a resistivity of 10^{-14} Ω-m

4.2.3.2 Other Magnets for the SSC

Although other superconducting magnets are needed for the collider and the high-energy booster, and conventional magnets are needed in the other parts of the injector complex and for special regions in the collider, it is beyond the scope of this summary to describe them. (Refer to Chapter 4 of the SCDR for a complete description.) Table 4.2.9 shows the quantities of the different types of superconducting magnets required for the SSC.

Table 4.2.9
Superconducting magnets required for the SSC accelerators

Collider dipoles	8652
Collider quadrupoles	2024
HEB dipoles	432
HEB quadrupoles	278

4.2.3.3 Cryogenic Systems

The SSC will apply superconductivity on a scale vastly larger than any before. An extensive cryogenic system is required to provide for the superconducting magnets during collider operation, during magnet cooldown and maintenance, and during quenches if they occur. The cryogenic system must be highly reliable to ensure availability of the SSC for research. Table 4.2.10 summarizes the general parameters of the SSC cryogenic system.

Table 4.2.10
Cryogenic system parameters

Operating temperature, coils	4.35 K max	
Operating temperature, refrigerator	4.1 K nom, 4.0 K min	
Total est. refrig. requirement (both rings and HEB) w/o redundancy and other allowances:		
4.15 K refrigeration	54.3 kW	
Synchrotron radiation	17.7 kW	
Other beam-related loss	4.1 kW	
Static heat leak	19.5 kW	
Other	6.9 kW	
Ramping load (HEB)	6.1 kW	
4.15-K liquefaction	290 g/sec	
20-K refrigeration	97 kW	
84-K refrigeration	660 kW	
Total liquid helium inventory	2.3×10^6 liters	
Number of arc refrigerators	10	
Arc refrigerator capacity	Nominal	Full
4.15-K refrigeration	5200 W	6500 W
4.15-K liquefaction	28 g/sec	35 g/sec
20-K refrigeration	9600 W	14400 W
Number of HEB refrigerators	2	
HEB refrigerator capacity	Same as collider	
Electric power summary (MW)	Nominal	Installed
Arc refrigerator		
Compressor (4160 V, 90% pf)	3.3	4.3
Auxiliaries (440 V, 70% pf)	0.5	0.5
Site power		
12 refrigeration plants	45.6	57.6
Heat rejection summary	Power	Flow
Refrigerator (water supplied at 90°F, returned at 105°F)	5.0 MW	2300 gpm
Storage capacity summary (gal)		
Helium		
Liquid	$20 \times 30{,}000$ (collider)	
	$2 \times 20{,}000$ (HEB)	
Gas (liquid, 89% of inv.; gas, 11% of inv.)	$110 \times 30{,}000$	
Liquid nitrogen (3-day supply at 2000 gal/s)	$11 \times 20{,}000$	

The extent of the SSC is such that a single centralized cryogenic system is not appropriate. Instead, a number of independent units will be employed for the collider and for the high-energy booster. However, although these units can operate separately, they will be interconnected for redundancy to help ensure reliable operation. The collider will have ten cryogenic units, with a cryogenic plant located at the midpoint of each of these cryogenic sectors. A helium refrigeration plant at each E area, about every 8 km along the collider, will cool 8 km of both superconducting magnet rings. Refrigeration equipment could be incorporated in the F areas if required as part of a future upgrade (for example, to increase the luminosity).

To cool the magnets, single-phase helium at 4.15 K and 3–4 atm will be fed into a 4-km string of magnets on either side of the refrigerator. It will flow through the magnets in series and be recooled periodically to maintain the operating temperature of 4.35 K or lower in all magnets. At the end of the string, the helium flow will be reversed and returned to the refrigerator.

The refrigeration plants must be able to provide the large amounts of cryogens needed to cool the magnets. For example, the liquid helium inventory in the collider magnets will be about 45,000 liters. In addition to providing for steady-state operation, the refrigeration plant must function effectively and reliably under a number of other conditions: cooldown of the magnets from ambient temperature to 80 K and then to about 4 K, warmup of part of the ring, and possibly operation at temperatures below the nominal operating temperature to condition the magnets. It may also be necessary to shift the load from one sector to another for repairs. Recovery from a quench, which dumps the helium inventory in a half-cell and raises the temperature to 20 K, must be as fast as possible.

4.2.3.4 Beam Instrumentation and Controls

An extremely precise and sophisticated control system is required to deliver beams of the right energy to the right place at the right time. Instrumentation and diagnostics will be needed not only during routine operation but also for commissioning and for studies aimed at improving machine performance. Diagnosis of faults that may occur is also a major function of the overall instrumentation and control system. Instrumentation and diagnostics elements for the many components in the accelerator complex are the sensing elements for the control system. Control hardware and software will be as similar as possible for every accelerator.

Beam instrumentation must measure beam position and intensity at many locations around the rings, measure the beam profile, and detect beam loss. A variety of instruments will be used. Beam-position monitors contain four electrodes: one above, one below, and one on either side of the beam. They will be located at most of the quadrupoles in all accelerators. By measuring and processing signals induced in each electrode, it will be possible to accurately measure and control the position of the beam. Beam-intensity monitors will measure the total circulating current in all rings. The transverse size of the beam will be measured at a few locations around each ring with flying wire scanners—which move a very thin wire at a known rate through the beam and use a detector to measure the interaction products—or with synchrotron radiation light monitors, routinely used in electron-positron colliders. Beam-loss monitors, simple gas-filled tubes sensitive to ionizing radiation, will be placed around the rings (about every 30 m in the collider) to detect radiation from beam losses. The monitors will both protect against radiation damage from beam loss and aid in tuning the machine.

Beam instrumentation, power supplies, vacuum systems, and cryogenic systems must all be monitored and synchronized. For many subsystems, local control will be needed during construction or maintenance. Personnel and equipment safety must be guaranteed at all

times, even if communication to a central control point is lost. Table 4.2.11 summarizes the number of monitor and control points in the accelerator complex.

The control system is made up of sensors connected to a hierarchy of computers. Information from local sensing elements is acquired, filtered, processed, and delivered to a higher-level computer for additional processing. Ultimately, the information is sent to human operators in the central control complex. A schematic view of the system architecture is shown in Figure 4.2.9.

Table 4.2.11
The number of monitor and control points in the accelerator complex

Collider	90,000
HEB	13,000
MEB	4,600
LEB	3,600
Linac	3,000
Test beams	1,700
Subtotal	115,900
Contingency	24,100
Total	140,000

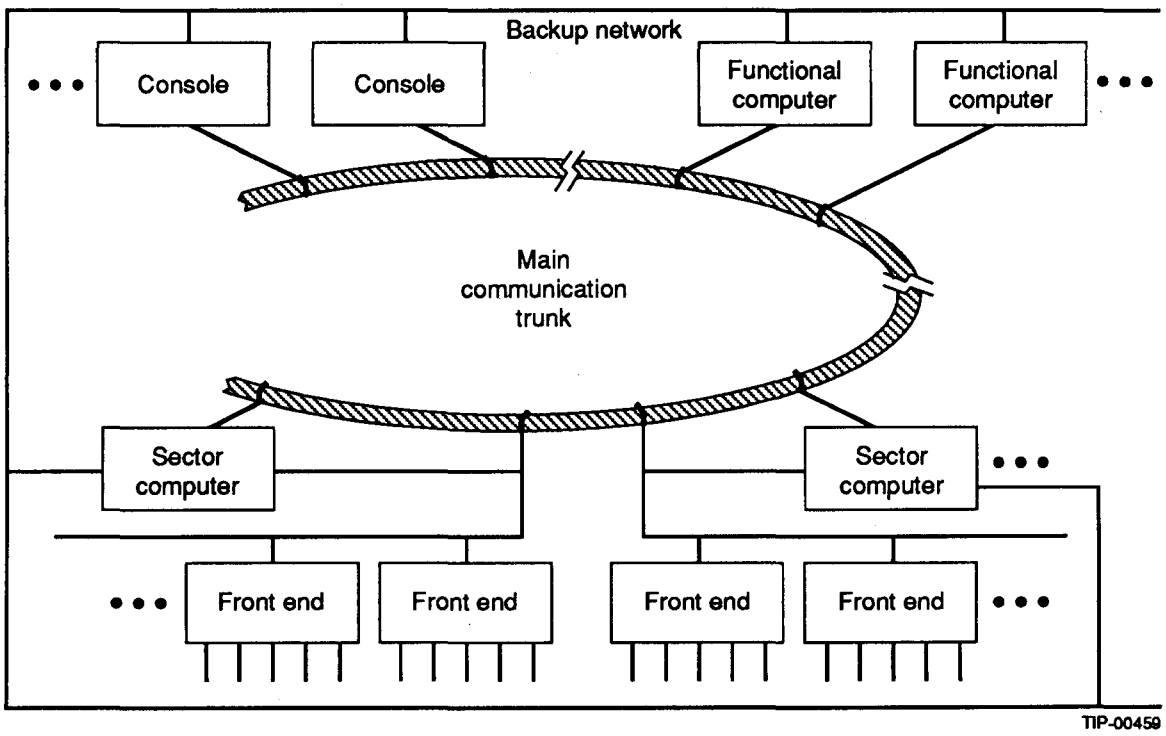

Figure 4.2.9 Schematic view of the computer architecture for the control system.

4.3 Experimental Systems

4.3.1 Introduction

In planning the SSC, it is important to provide for experiments that will explore the new energy domain of the SSC as thoroughly and thoughtfully as possible. Since the initial experimental program will not be defined completely until some years hence, a plausible model of experimental systems (based on extensive workshops and summer studies of possible SSC experiments) has been developed to allow estimates of costs and construction schedules. This model should not be considered a description of the final nature of the initial SSC experimental program. That will be determined by a process described in subsection 4.3.2.2.

Experimental systems at the SSC comprise the experimental apparatus, the underground halls and surface buildings that house and support the experimental program, utilities to operate the halls and support buildings, and external beams to test and calibrate detector components.

A schematic layout of the interaction regions is shown in Figure 4.3.1. Collider experiments may be done in four interaction regions: two on the east side of the collider ring and two on the west side. Bypasses around both east and west clusters will not be bored nor instrumented as part of the initial configuration of the SSC, but, once constructed, they would allow up to four additional interaction regions to be built with minimal impact on running experiments.

4.3.2 Experiments at the SSC

This section treats the general scope of the initial SSC experimental program and the procedures that will be used to determine it.

4.3.2.1 Scope of the Initial Experimental Program

In an ideal world, the initial experimental program would provide for all possible physics results that might be observed at the SSC. (In practice, of course, this goal is not attainable, since much of the physics that will result from SSC operation cannot be predicted.) The experimental goals of the initial program, which seeks to come as close as possible to the ideal in the real world, may be broadly classified as follows:

- high-P_t physics; exploration of mass scales from about 100 GeV/c^2 to the multi-TeV/c^2 range, investigations of electroweak symmetry breaking and discovery of new particles;
- studies of known particles (for example, hadrons containing b quarks) copiously produced at the SSC;
- studies of quantum chromodynamics at previously unobtainable energies;
- systematic studies of processes that occur with large cross sections, including total cross section measurements; and
- searches for truly exotic unpredicted processes that could substantially change the existing model of high-energy physics.

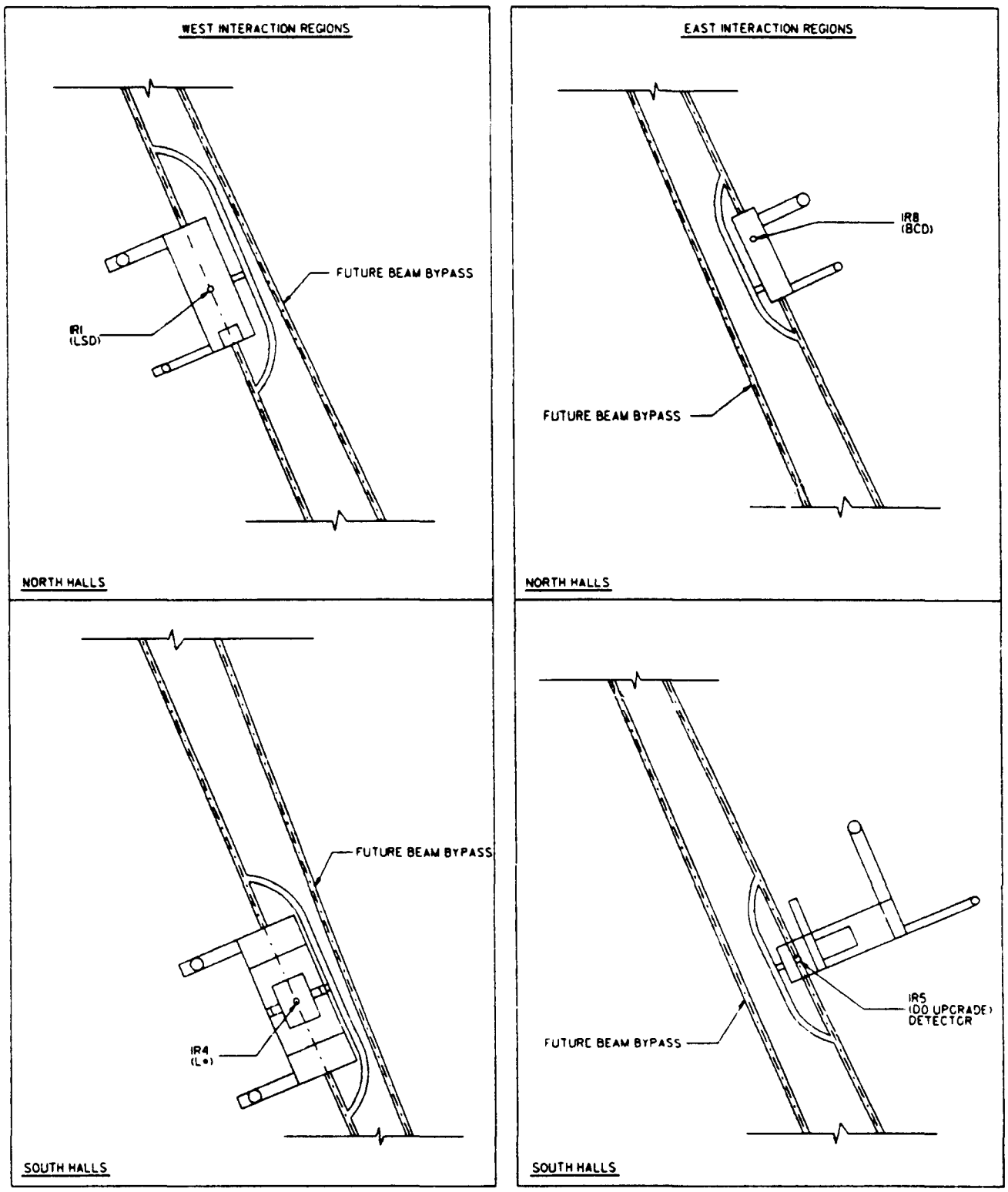

Figure 4.3.1 Schematic layout of the model of experimental halls used to determine experimental support requirements. (Note that the detectors shown here are for illustrative purposes only and do not reflect final decisions about actual experiments in the initial experimental program.)

Meeting these goals requires a variety of experimental systems. Experiments designed to explore high-P_t phenomena are characterized by the need to measure the energies and directions of high-energy particles produced in violent collisions and thus must be large in size. Experiments designed to measure the detailed decay properties of B mesons or to observe CP violation in B decays will be more modest in size, similar to that of the current generation of experiments, such as CDF and D0 at the Fermilab Tevatron. Experiments to study processes with large cross sections are still smaller. Experiments to observe exotic particles or signatures may vary in size from very small to medium.

The SSC Laboratory is dedicated to fostering a diverse experimental program, one that is not only responsive to today's physics goals but also flexible enough to adapt to future discoveries or developments in particle physics. The initial SSC experimental program will include one or more new large detectors to explore in detail high-P_t phenomena and the frontier of physics opened by the SSC. The number and nature of these detectors will be determined in the next few years. Smaller experiments requiring less time to design and build may be approved for initial operation on a somewhat longer time scale.

4.3.2.2 Procedures to Establish the Experimental Program

The SSC Laboratory will follow the usual procedures of existing high-energy physics laboratories in determining its experimental program. Experiments will be initiated by expressions of interest (similar to letters of intent) or proposals submitted to the Laboratory. These will be reviewed in detail by a Program Advisory Committee (PAC) for physics merit and technical feasibility and by Laboratory staff members for impact on Laboratory resources. Recommendations from these groups will then be presented to the Director.

An international Program Advisory Committee advises the Director. This Committee first met in February 1990 to determine the procedures and schedule for evaluation of the first round of SSC experiments. The schedule is given in Table 4.3.1. Beyond November 1990 the schedule is tentative; it will be firmly established in further PAC meetings.

Expressions of interest represent the first formal step in defining the experimental program. Longer than traditional letters of intent but less detailed than proposals, they will be used to determine support for experiments whose design and construction must begin now if they are to be ready when the accelerator is. More detailed proposals based on this preliminary work can then emerge by the end of 1991.

Table 4.3.1

Schedule through 1991 for determining the initial SSC experimental program

First meeting of PAC	February 1990
Expressions of interest due	May 25, 1990
Expressions of interest presented to PAC	June 7–9, 1990
Expressions of interest reviewed	July 1990
Expressions of interest recommended	November 1990
Meeting of PAC	July 1991
First proposals due (tentative)	Last quarter 1991

4.3.2.3 Determination of Experimental Support Requirements

Based on extensive workshops and summer studies of SSC detectors over the last few years, a scenario of the initial experimental program has been developed to determine requirements for experimental support systems. This scenario does not necessarily reflect

precisely the final choices that will be made about the initial experimental program. It merely presents a plausible range of requirements for a robust experimental program at four interaction regions. The model also attempts to anticipate the requirements of a later experimental program, particularly the desirable underground hall features.

SSC experiments can be roughly grouped into four categories, as shown in Table 4.3.2. This categorization is useful in defining the space requirements for underground halls. (Very small experiments may be housed in the collider tunnel.)

Table 4.3.2
Categories of possible SSC experiments used in estimating experimental hall size and support systems requirements.

Large	General-purpose, 4π detectors designed specifically for the SSC. These detectors will be significantly larger than existing 4π detectors and will operate at or just below maximum collider luminosity.
Medium	Upgrades of existing 4π detectors and new detectors of more modest size.
Small	Particle searches and survey experiments, modest in size and duration compared with large or medium experiments. These detectors will vary widely in their luminosity requirements, from the design maximum to many orders of magnitude less.
Very small	Total cross section and other experiments that require minimal space and a wide range of luminosities.

Since 1984, many potential SSC experiments have been described. Most of these are large or medium experiments of similar character. Since, for these purposes, many of these detectors are alike, detailed support requirements have been developed based on representative detectors. The Large Solenoidal Detector (LSD) and the L* concept were chosen as guides to the needs of large detectors. The Bottom Collider Detector (BCD) and the D0 upgrade were chosen as representative medium detectors. (The origins of these detector concepts are given in Chapter 5 of the SCDR.)

The layout of experimental halls based upon this model is shown in Figure 4.3.1. The two large halls are located on the outer leg of the bypass configuration in the west cluster; the two medium halls are on the outer leg in the east cluster. This arrangement maintains approximate equality in the luminosity of neighboring interaction regions, which is desirable for beam stability. This plan is also economical: due to different soil conditions, the cost of excavation per unit volume on the west side is significantly lower than on the east side.

4.3.3 Interaction Regions

Two principal types of interaction region optics have been designed:

- a low β^*(β^* = 0.5 m), high-luminosity (that is, design luminosity) region with a free space of ±20 m (or less if desired) about the interaction point; and
- a medium β^*(β^* = 10 m), medium-luminosity region with a longer possible free space up to ±100 m about the interaction point.

The layout of the optics for a low β^* region is shown in Figure 4.3.2. The layout of a medium β^* region would be similar except for the additional free space for experiments.

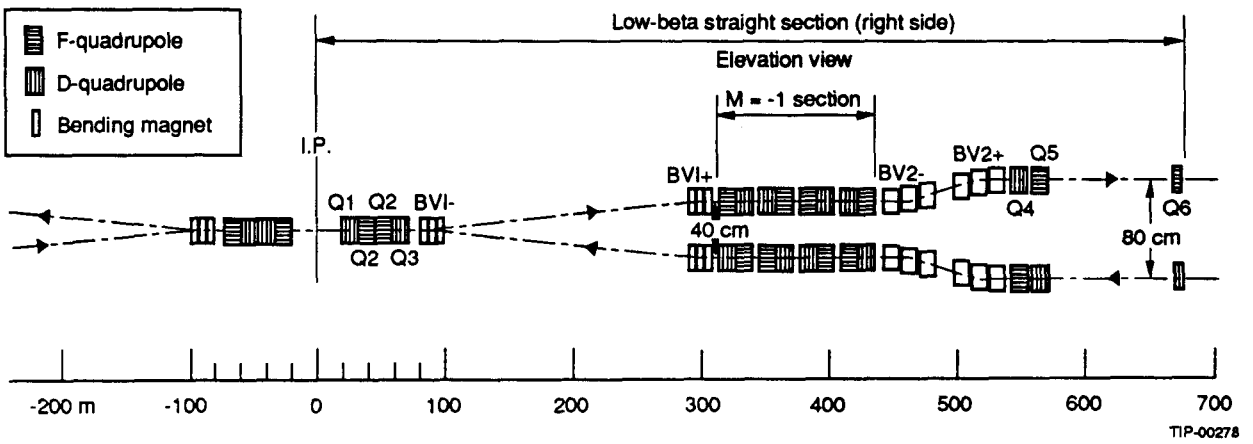

Figure 4.3.2 Elevation view of a low-β^* interaction region.

It is advantageous to have two identical or nearly identical optical regions in each cluster. Preferably, then, two high-luminosity regions will be located in the west cluster and two medium-luminosity regions in the east cluster. But pairing is not absolutely required; the substitution of one low β^* region in the east cluster will be considered if necessary. Additional interaction region optics (i.e., to accommodate measurements of the proton-proton total cross section) have also been considered. The precise arrangement of interaction optics can only be specified after the nature of the SSC experimental program has been determined.

4.3.4 Experimental Plant and Utility Requirements

The plant and utility requirements for constructing and operating experiments, including the underground halls in which the experiments will be housed and the surface buildings in which the apparatus will be assembled and operated, have also been estimated.

The size of underground experimental halls is determined by the size of the detector and by assembly and maintenance requirements. For each of the four detectors in the model, a preliminary study has been made that considers in detail the dimensions, weights, and assembly procedures of the major detector components. An example, the components for the Large Solenoidal Detector, is shown in Figure 4.3.3.

Two varieties of large halls have been designed. (See Figures 4.3.4 and 4.3.5.) Type A is the model for the northwest experimental area; Type B is the model for the southwest area. Any of the large SSC detectors considered so far can fit into one of these halls.

Two smaller halls, comparable to underground halls at existing accelerators, have been designed for the east cluster. One hall was modeled to house the Bottom Collider Detector, an experiment that would require more free space than the large detectors but is otherwise smaller. The other medium underground hall in the east cluster was used as a model for an upgrade of the D0 detector, but it could house many other smaller experiments. The basic dimensions of the these halls are summarized in Table 4.3.3. Detailed descriptions of the halls are given in Chapter 5 of the SCDR.

All of the underground halls as modeled would be constructed using open-pit techniques. Because the ratio of excavation to completed hall volume would be substantially larger in the east cluster (soil conditions there require a larger slope-back during open-pit excavation), the large halls are placed in the west cluster.

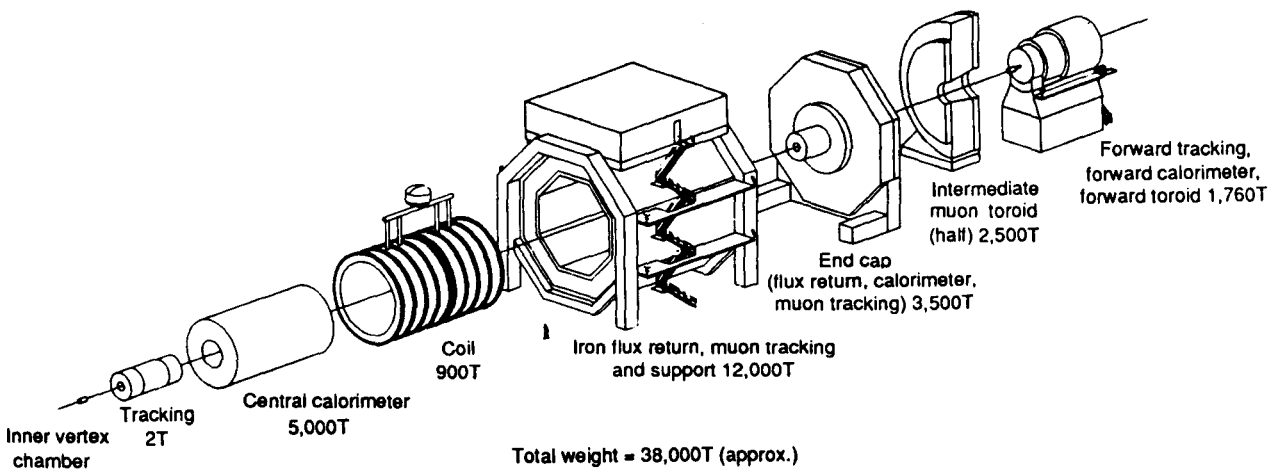

Figure 4.3.3 Exploded view of the Large Solenoid Detector showing major components.

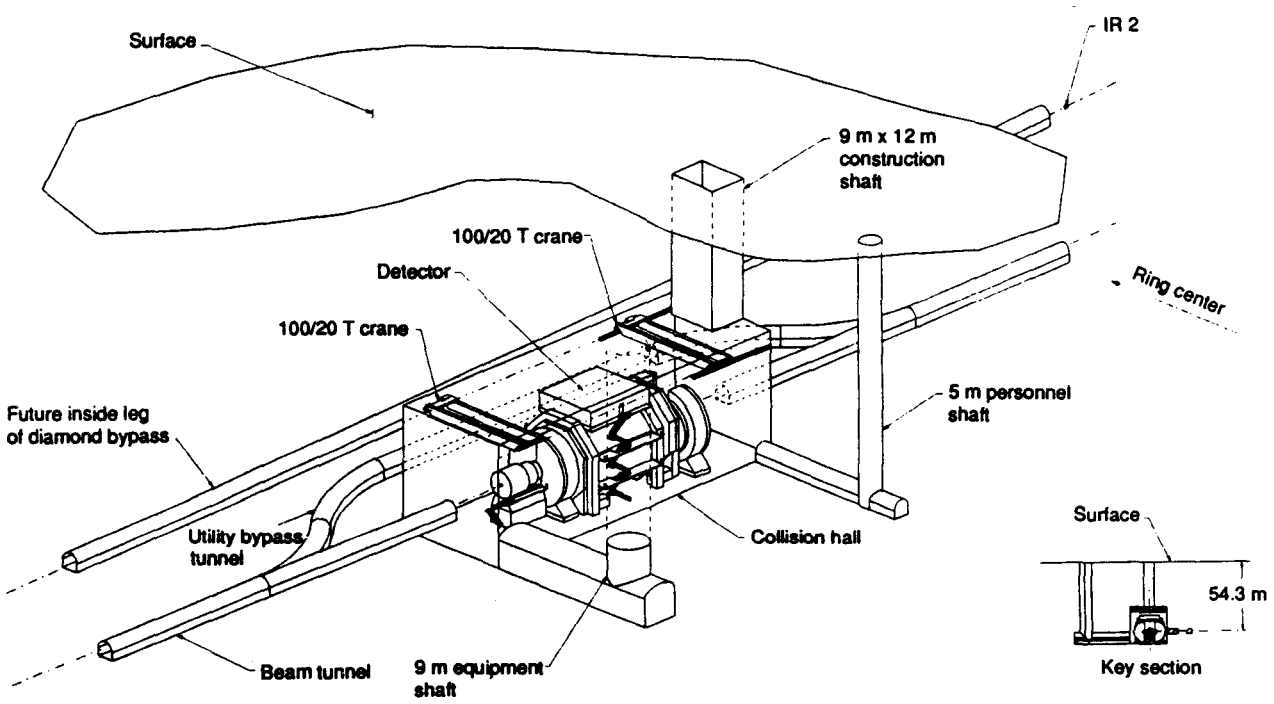

Figure 4.3.4 Isometric view of a Type A underground hall. It was designed on the basis of the Large Solenoid Detector but could house other detectors of comparable size and scope.

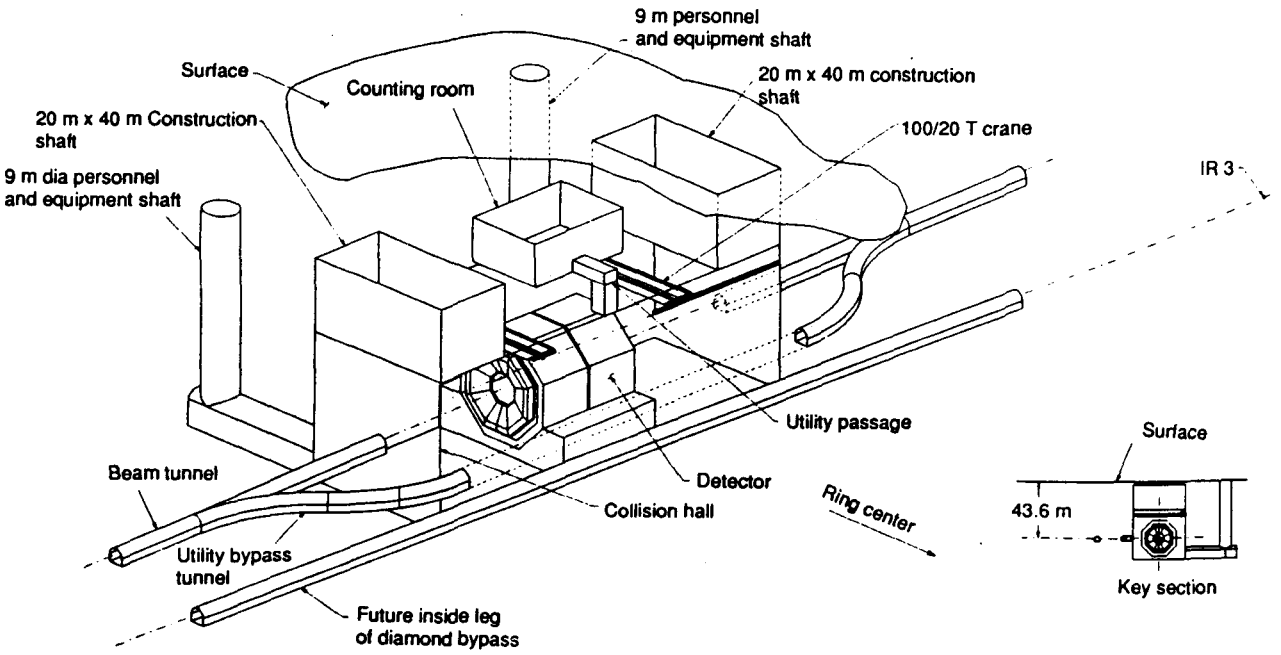

Figure 4.3.5 Isometric view of a Type B underground hall. This hall was designed on the basis of the L* detector but could also house other detectors of similar size and scope.

Table 4.3.3
Dimensions of model underground halls.

Interaction Region	Depth to Beam (ft)	Type of Hall	Length (ft)	Width (ft)	Roof Height (ft)
1	183	Large – A	262	92	95
2	171	Future	—	—	—
3	133	Future	—	—	—
4	140	Large – B	354	131	123
5	154	Medium – B	161	75	79
6	153	Future	—	—	—
7	129	Future	—	—	—
8	138	Medium – A	197	59	66

A variety of surface structures will support operations in the underground halls, provide assembly space for experimental apparatus, and house participants in the experimental program. The space needed to assemble apparatus, the utilities requirements, and the number of people required to assemble, install, maintain, and operate the experiments have all been estimated.

In the west cluster, a common industrial-type area is provided about midway between the north and south experimental areas. This area contains general-purpose industrial buildings for detector assembly and allows for buildings suited to special purposes, such as construction of a large superconducting coil. An operations complex for control of test beams and some aspects of the interaction regions would also be located in this general area.

A preliminary estimate of power, water, and other utilities requirements for SSC experiments has been made and is documented in Chapter 5 of the SCDR.

4.3.5 Test Beams

In the initial configuration, a 200-GeV beam from the medium-energy booster will be extracted and transported to target stations, creating three secondary beams for test and calibration of experimental equipment. A schematic view of the relationship of the test beam area to the medium-energy booster, high-energy booster, and collider is shown in Figure 4.3.6. A more detailed view of the test beam layout is given in Figure 4.3.7. The secondary beamline design is based on the wide-band photon beam at Fermilab. The secondary beamlines will be able to deliver hadron beams from about 1 GeV up to the full 200 GeV of the medium-energy booster. Tagged electrons with usable rate will be available from 1 GeV up to about 100 GeV.

The test beam facility will be designed to allow for a later upgrade to include beams derived from the high-energy booster or additional beamlines. Stubs for a future access tunnel from the high-energy booster, which is almost as deep as the collider, to near the surface will be constructed as part of the initial configuration. This step will allow much of the transport system from the high-energy booster to target stations and secondary beamlines to be constructed with minimal interference to operations of the high-energy booster and collider. Surface calibration halls will be designed with this possible upgrade in mind.

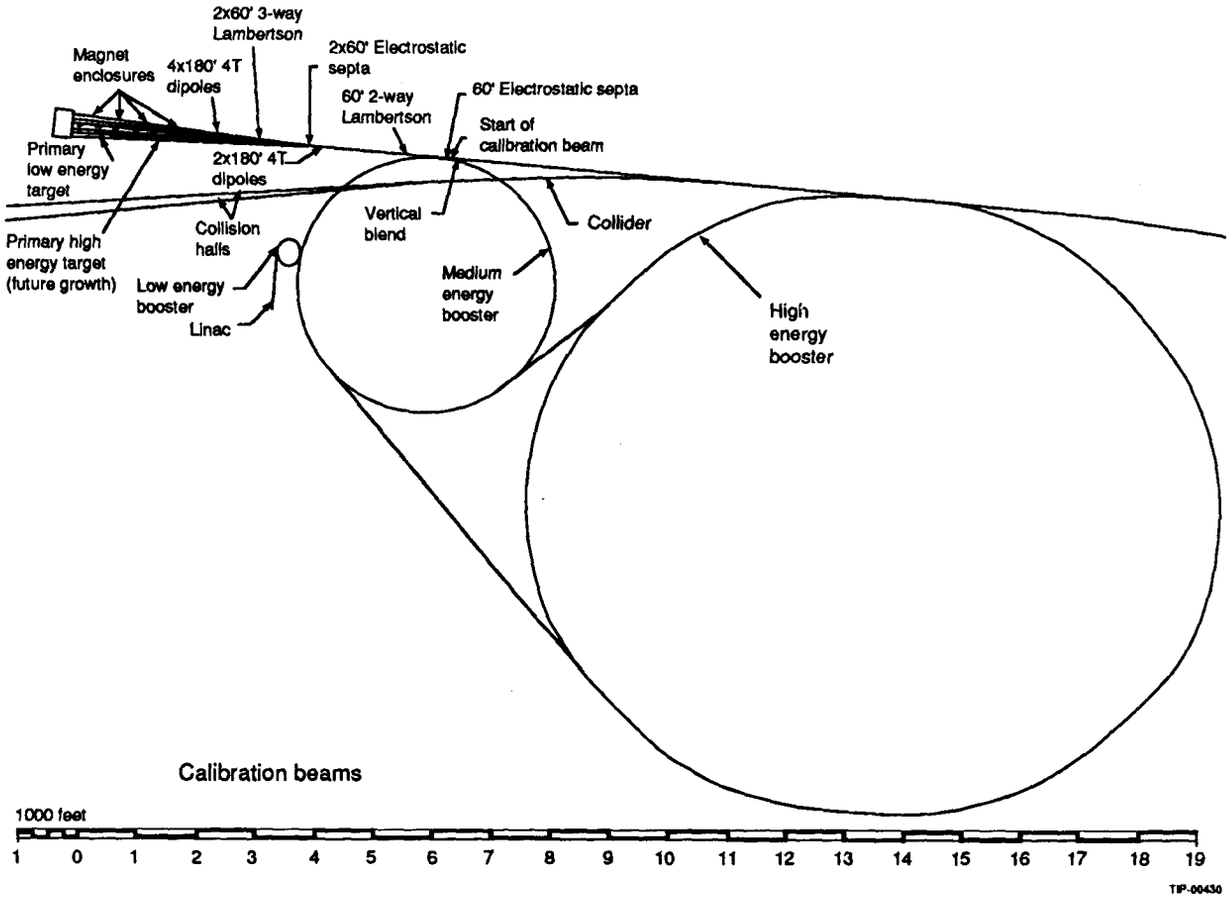

Figure 4.3.6 Schematic view of the layout of the test beam area.

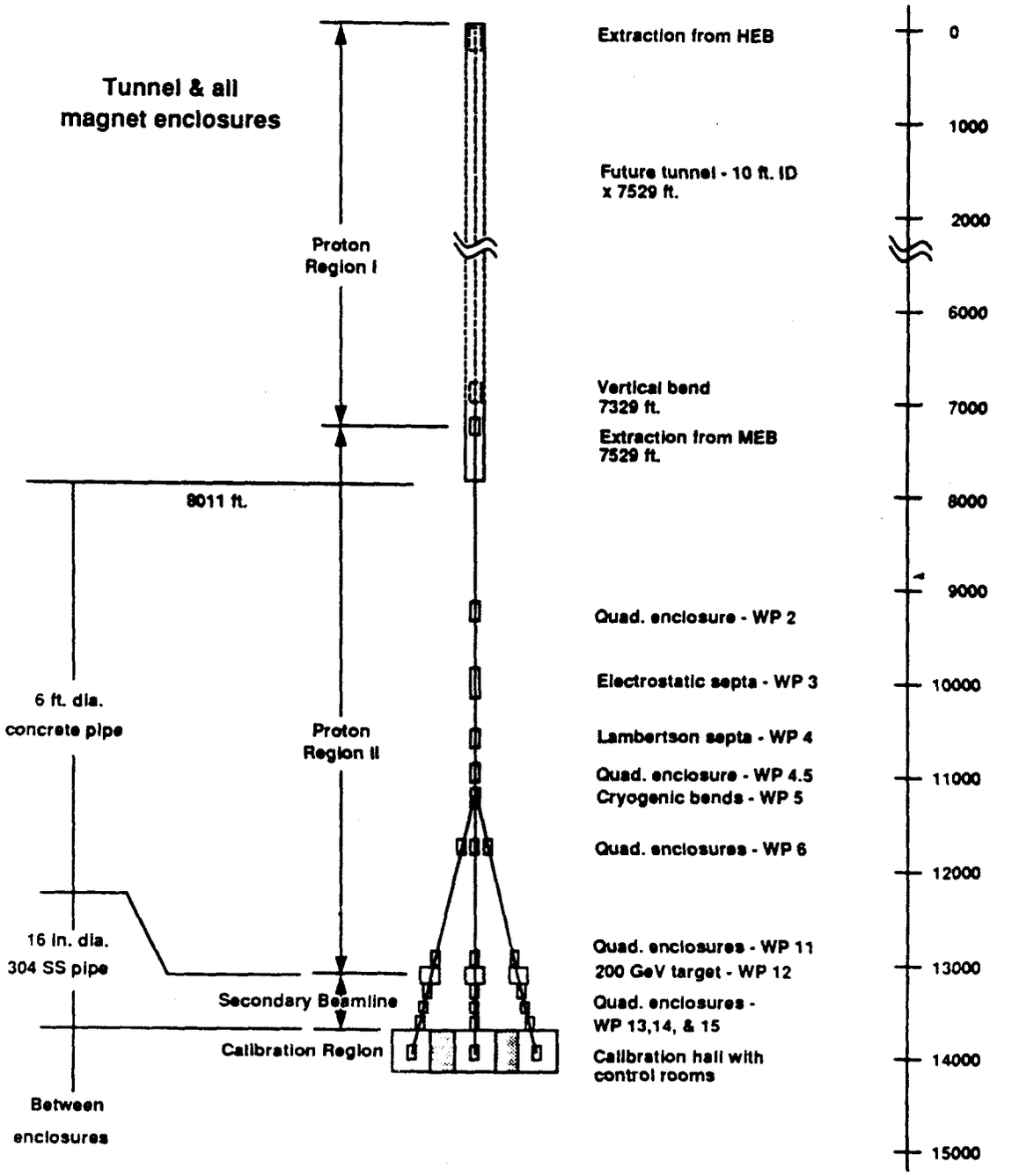

Figure 4.3.7 A plan view of the test beam optics layout. Only secondary beams from the medium-energy booster will be available in the initial configuration of the SSC, but provision for an upgrade to include beams derived from the high-energy booster will be made.

5. Operations

5.1 Operations Cycles

Initial operation of the accelerators in the SSC complex will occur sequentially, culminating in operation of the collider. (The schedule for construction of the injector accelerators is discussed briefly in Chapter 6.) Conceptually, collider operation may be divided into four time periods: initial commissioning, initial operation for experiments with gradual improvements in reliability and performance, sustained operation for experiments, and upgraded operation. (Possible upgrades are discussed in Section 5.2.)

The injector complex will function in two modes: injecting beam into the collider and providing external beams (initially from the medium-energy booster and later from the high-energy booster) to the test beam area. The eventual standard cycle times for the accelerators are summarized in Table 5.1.1. A complete high-energy booster cycle takes about 2 minutes, and filling one of the collider rings takes about 15 minutes, so the total filling time for both rings will be about 30 minutes plus the time required to reverse polarity of the high-energy booster and to tune up the transfer lines. At design luminosity, the storage time in the collider rings will be about one day. A more detailed description of the cycles for filling one of the collider rings is given in Figure 5.1.1.

Table 5.1.1
Cycle times for the injector and the collider

Accelerator	Mode	Cycle Time
Linac	Injector	0.1 sec
LEB	Injector	0.1 sec
MEB	Injector	3.0 sec
	Injector (coalesced)	3.5 sec
	Test beams	4–5 sec
HEB	Injector	2.0 min
	Test beams	~3.0 min
Collider	Collider	~24 hr

5.2 Future Options

To be able to respond to new physics discoveries and to increase the physics reach of experiments, experience suggests that the effective luminosity delivered by the collider must improve with time, or that existing experiments must be upgraded or completely replaced. The design of the SSC facilities takes into account all of these possibilities and provides substantial potential for improvements to keep the Laboratory at the forefront of science long after the first physics results are reported.

(a)

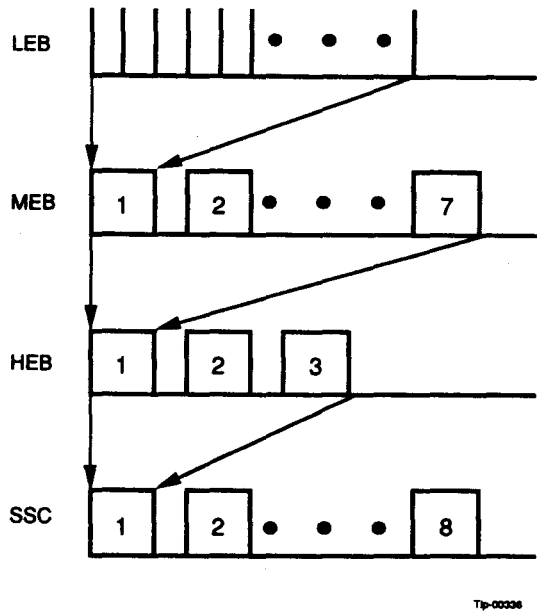

(b)

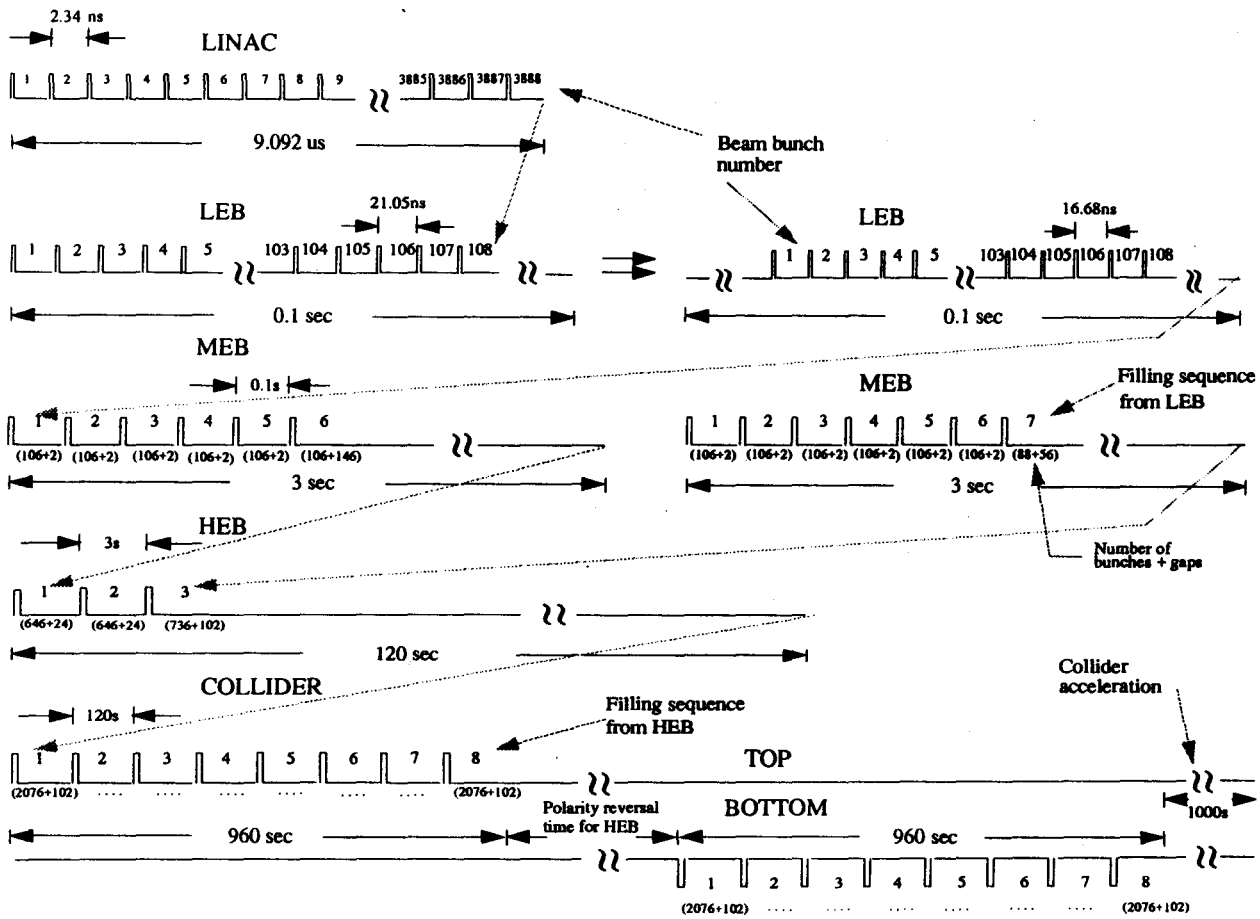

Figure 5.1.1 The filling sequence from the low-energy booster to the collider: (a) general, (b) more detailed look at the relevant times.

5.2.1 Beam Bypasses

Bypasses represent one opportunity for future expansion and versatility in the experimental program. The clustered interaction regions have a diamond-shaped bypass arrangement, shown in Figure 5.2.1. Each outer leg consists of two interaction regions separated by a segment that closes the loop of the collider ring. The outer legs will be fully operational in the initial configuration of the SSC. The inner legs, to be constructed later, have an additional region of reverse bend and equal compensating regions of bend in the direction of the arcs to close the machine. The path lengths would be equal in both legs.

Implementation of one or both bypass arrangements offers two important advantages. First, operation of the collider in one leg would be decoupled to a very large extent from maintenance and repair of experiments in the other leg. Second, additional interaction regions could be constructed along the inner bypass legs with minimal interference to collider operations or to experiments in the outer leg.

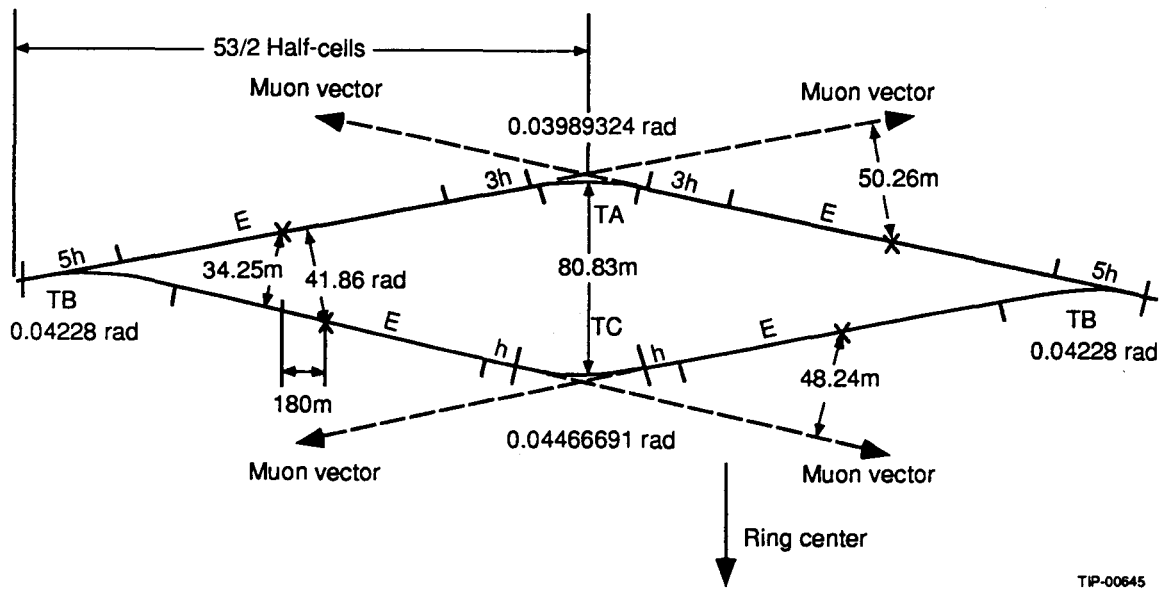

Figure 5.2.1 The diamond bypass arrangement. In the initial configuration, the outer legs (farther from ring center) will be instrumented.

5.2.2 Experiments Beyond the Initial Complement

Funds allocated for the initial complement of detectors will provide for an experimental program that is capable of realizing the major scientific goals of the SSC. However, as the first SSC experiments mature and new discoveries are made, the need to either upgrade existing detectors or to build new experiments may become apparent. In addition, as discussed in more detail in the next section, the luminosity of the SSC is likely to increase with time, creating additional challenges to detector technology that may only be met with new or improved apparatus and techniques.

5.2.3 Increased Luminosity

The physics capabilities of a colliding-beam accelerator are ultimately limited by the integrated luminosity that experiments can accumulate. Although some improvements in

operational reliability can usually be made, the peak collider luminosity finally limits the physics reach. As the proton beams in the collider are brought into collision, the luminosity will increase as the result of both the complex interaction of the two beams with each other and a host of single beam effects. For the parameters given in Table 5.2.1, the luminosity will evolve as shown in Figure 5.2.2, starting at the design value of 10^{33} cm^{-2} sec^{-1}. At this value, about 1.5 proton-proton interactions will occur on average at each crossing.

Table 5.2.1

Beam parameters that influence luminosity at the design luminosity of 10^{33} cm^{-2} sec^{-1}

Initial normalized emittance	1.0 π mm-mrad
Initial emittance growth rate due to	
Intrabeam scattering	5.4×10^{-17} mrad/sec
Residual gas scattering	7×10^{-17} mrad/sec
Beam-beam	ignored
Collective instabilities	ignored
Elastic pp collisions	4×10^{-17} mrad/sec
Synchrotron radiation damping	-1.03×10^{-15} mrad/sec
Initial particle loss rate due to	
Inelastic pp collisions	1.1×10^{4} protons/sec
pp bremsstrahlung	40 protons/sec
Touschek scattering	43 protons/sec
Residual gas scattering	6500 protons/sec
Collision lattice	2 high- and 2 medium-luminosity IPs

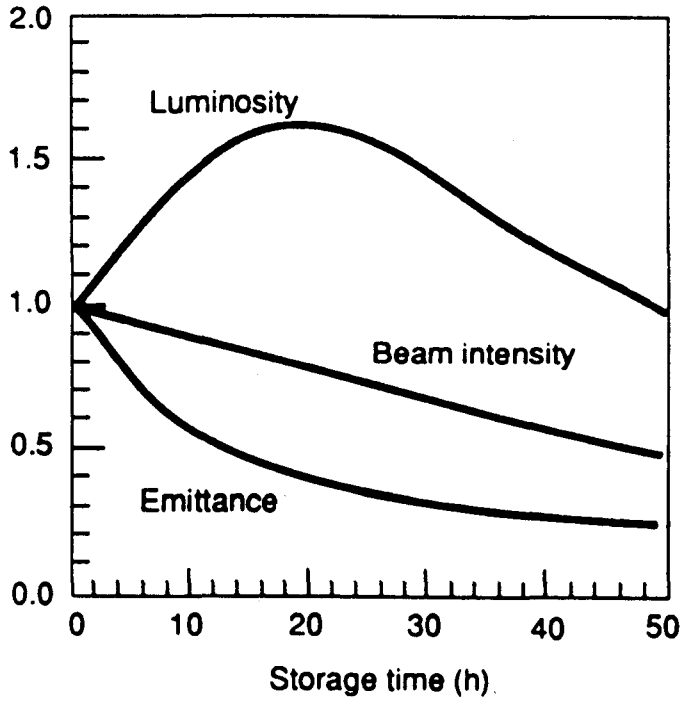

Figure 5.2.2 Collider luminosity, beam intensity, and emittance as a function of time for the parameters given in Table 5.2.1. The value of 1.0 on this scale corresponds to the design values (10^{33} cm^{-2} sec^{-1} luminosity).

No fundamental accelerator physics issues limit the luminosity of the collider to 10^{33} cm^{-2} sec^{-1}. This value was chosen as the design luminosity based on general-purpose detector capabilities, already significantly challenged at this luminosity, and because of the desire to keep the number of interactions per bunch crossing close to unity. It is very likely that, as detector technology improves and experience is obtained in handling multiple interactions within the same crossing, exploiting increased luminosity will become possible. Even now it is apparent that a limited class of special-purpose detectors (such as those that only detect muons behind a significant absorber) are feasible at luminosities substantially greater than 10^{33} cm^{-2} sec^{-1}. However, many technical issues must be considered carefully to allow for higher luminosity operation. These include the effect on vacuum in the collider from an increased synchrotron radiation load, increased energy deposition in magnets and scraper systems, increased radiation damage to components in the collider tunnel, and beam instability problems.

The collider luminosity could be increased in a number of ways, discussed in some detail in Chapter 4 of the SCDR and in an SSC internal report.[7] The parameters for two different scenarios to increase the luminosity are summarized in Table 5.2.2. In both cases the initial luminosity reaches 10^{34} cm^{-2} sec^{-1}, but there are substantially different values for the number of events per crossing.

Table 5.2.2
Parameters for three possible collider operating scenarios

	Nominal	Scenario 1	Scenario 2
Initial values			
Luminosity (cm^{-2} sec^{-1})	1.0×10^{33}	1.0×10^{34}	1.0×10^{34}
Protons per bunch	7.0×10^{9}	2.2×10^{10}	7.0×10^{10}
Bunch spacing (m)	5.0	5.0	50
Events per collision	1.5	15	150
Synchrotron radiation (kW)	8.5	27	8.5
Crossing angle (μrad)	75	94	129
Beam-beam tune shift			
Head-on/IP	0.00086	0.0027	0.0086
Long range/IP	0.0020	0.0040	0.00068
Total	0.0078	0.020	0.036
Peak values			
Luminosity (cm^{-2} sec^{-1})	1.6×10^{33}	1.0×10^{34}	1.0×10^{34}
Events per collision	2.4	15	150
Beam-beam tune shift			
Head-on/IP	0.0018	0.0033	0.0086
Long-range/IP	0.0020	0.0040	0.00068
Total	0.0105	0.020	0.036

Luminosity also depends on beam energy. The limitations that have been considered include the head-on beam-beam tune shift limit, the long-range beam-beam limit, and synchrotron radiation power per unit length. If the cryogenic capacity can be increased by a factor of four above the nominal design value to handle a synchrotron power of 0.4 W/m, the maximum luminosity would occur at a beam energy of about 18 TeV and would exceed 10^{34} cm^{-2} sec^{-1} even at 20 TeV. (See Figure 5.2.3.). Even if the cryogenic capacity is kept at the nominal value to handle 0.1 W/m, the peak luminosity could exceed 10^{34} cm^{-2} sec^{-1}.

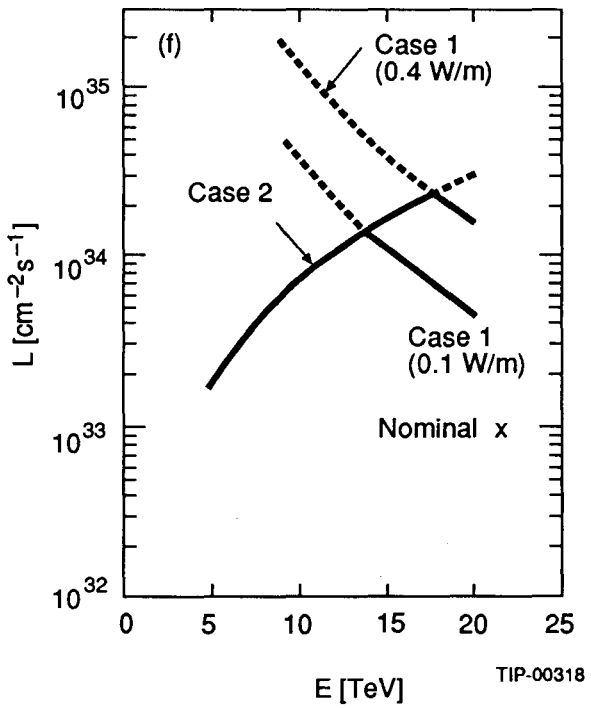

Figure 5.2.3 Luminosity of the collider assuming a total head-on beam-beam tune shift of 0.01 and a long-range beam-beam limit of 0.005 for each of two high-luminosity regions. Two different cryogenic capacities to handle synchrotron radiation power, 0.4 W/m and 0.1 W/m, are considered. The nominal design value for the collider is 0.1 W/m. Increased cryogenic capacity would be required for 0.4 W/m operation.

6. Project Status and Outlook

The completion of the Site-Specific Conceptual Design Report (SCDR) is a major step in the SSC project. The Design Report and supporting documentation present a complete conceptual design and related cost and schedule estimates for all aspects of the SSC. The land required for the accelerators and the experiments has been determined, and the process of acquiring it has begun. All major accelerator parameters have been fixed, and detailed design leading to construction of the accelerator components is beginning. An aggressive program of collider dipole magnet development will lead to production of the first collider dipoles in collaboration with industry and to a test of a string of dipoles under conditions similar to SSC operation by the end of fiscal year 1992. Conceptual plans for civil construction associated with the accelerators and the experiments now exist and have been documented in the SCDR. In the summer of 1990, the AE/CM consortium of Parsons-Brinckerhoff/Morrison-Knudsen will begin to work with Laboratory staff to turn the conceptual designs into reality. Procedures to initiate the experimental program at the SSC have been established, and expressions of interest in SSC experiments will be reviewed in the summer of 1990.

In the sections below, plans for the next two years are described in greater detail, and the schedule for major aspects of the project is presented. Of course, much more information exists about the near-term plans for the SSC and about the project cost and schedule; the companion documents to the SCDR should be consulted for details.

6.1 Goals of the Next Two Years

The major goals of the SSC Laboratory for accelerator systems, magnet systems, and the experimental program in the next two years are presented below. The most important objective of the accelerator and magnet programs is to build and test a substantial number of collider dipoles and associated components in a realistic environment. The central aim of the experimental program is to approve and initiate the design and construction of the first major SSC experiments.

Accelerator Systems Goals

1. Design and construction of the accelerator systems string test (ASST) facility at the E1 sector service area. This surface-level testing area will be used for magnets and related systems. During fiscal year 1992, the goal is to test a half-cell of magnets and components. Longer magnet strings will be tested in later years.
2. Design and construction of a prototype installation facility (PIF), also at the E1 area. This underground test area will be used to gain crucial geological information and to test the design of shafts and the collider tunnel. The goal is to test a half-cell of magnets and related components underground, after they have been tested at the surface, by the end of fiscal year 1992. The PIF will allow testing of

all aspects of assembling and operating a magnet string under even more realistic conditions than the ASST.

3. Significant expansion of the detailed design of the linac, the low-energy booster, and the medium-energy booster. Magnet prototypes for the low-energy booster and medium-energy booster will be built in fiscal year 1991. Procurement of most linac components will be completed and housing for the linac will be nearly complete by the end of fiscal year 1992. A conceptual design of the high-energy booster will also be completed.

Magnet Systems Goals

1. Production of collider dipole magnets with a 50 mm aperture. This is the highest priority of the magnet program. A series of short magnets with 50 mm apertures will be built at Brookhaven and Fermilab during fiscal year 1991. Two full-length 50-mm aperture magnets will be completed by the end of fiscal year 1991.
2. Selection of an industrial contractor for the collider dipole magnets by the fall of 1990. The contractor will work with the staff from the SSC and other laboratories to prepare the collider dipole magnet design for industrial-scale production. The contractor will also assemble twelve full-length dipoles to be tested by the end of fiscal year 1992.
3. Accelerated life tests of collider dipoles. Reliability will be tested by rapid magnetic and thermal cycling of a number of full length dipoles. These tests will start with one magnet this summer and proceed to short magnet strings. These initial tests will be completed in fiscal year 1992.

Experimental Program Goals

1. Evaluation of the first expressions of interest in experiments by early fiscal year 1991.
2. Completion of the detector technology research-and-development program on major subsystems of potential experiments by the end of fiscal year 1992.
3. Initiation of conceptual design studies and preliminary engineering design work leading to detailed proposals for experiments by early fiscal year 1992.
4. Approval of the construction of one or more major experiments in fiscal year 1992.

A primary goal of the Laboratory will be to increase the number of personnel in all areas to carry out the design and begin construction of major project components.

6.2 Cost Summary

The cost of the SSC project has been estimated by the Laboratory staff and presented recently to the Department of Energy during a review of the SSC site-specific conceptual design.[8] The overall cost is to be determined in the near future, and is expected to be about $8 billion. Of the total costs, 25% is for R&D and the development of the initial detectors. The fabrication of the technical components including the superconducting magnets represent approximately 55%. Finally, 20% of the costs are for the facilities to house laboratory personnel, the enclosures for accelerator components, and the experimental halls for the research detectors.

6.3 Schedule Summary

A summary of the (draft) SSC construction schedule as presented at the DOE review of the SSC site-specific conceptual design is shown in Figure 6.3.1. Major milestones as presented are shown in Table 6.3.1. Schedules for the design and construction of each major subsystem have been established, and the interdependencies of various subsystems have been examined in detail. An aggressive effort is planned to design and build the linac, the low-energy booster, and the medium-energy booster by the end of 1995, to provide test beams on site for experimenters. This will also provide early experience with accelerator operations and control systems. The construction of the largest underground halls to house experiments will also be completed at the end of 1995, so that installation of complex apparatus may begin soon afterwards. Construction of the collider tunnel is planned to begin in 1991 and be completed by late 1996. It is planned that the SSC construction will be completed by the end of 1998, and experiments will commence following collider commissioning.

Table 6.3.1
Major project milestones – preliminary

Number	Name	Date	
M1-1	A/E award	May	90
M1-2	Baseline validation complete	July	90
M1-3	Collider dipole magnet (CDM) contract award	Aug	90
M1-4	SEIS record of decision	Nov	90
M1-5	Start SSC civil construction	Jan	91
M1-6	Collider string test complete industry prototypes	Oct	92
M1-7	Start first sector CDM delivery	Oct	93
M1-8	Begin excavation of experimental halls	Mar	93
M1-9	First collider sector – start installation	Jan	94
M1-10	Linac – start commissioning	Oct	94
M1-11	First sector – start cooldown	May	95
M1-12	MEB – start commissioning	Oct	95
M1-13	Beneficial occupancy of large experimental halls	Oct	95
M1-14	HEB – start installation	Jan	96
M1-15	MEB – test beams available	Apr	96
M1-16	HEB – start commissioning	Oct	97
M1-17	Detectors – start commissioning	Mar	98
M1-18	Collider – start commissioning (beam)	July	98
M1-19	Collider – complete commissioning beams to experiments	Oct	98

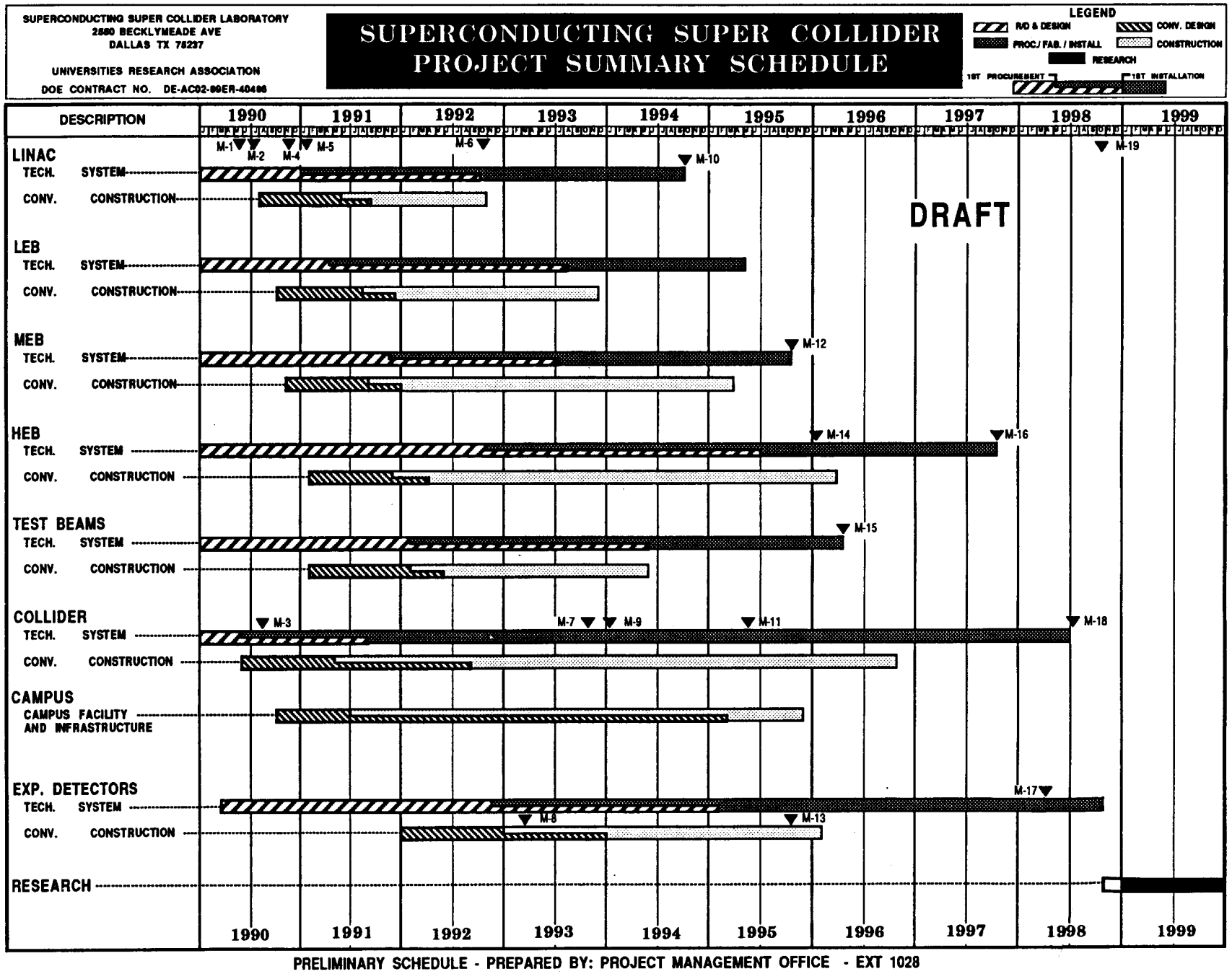

Figure 6.3.1 The SSC construction schedule.

References

1. Superconducting Super Collider Site-Specific Conceptual Design, SSC-SR-1051, July 1990.

2. For a comprehensive summary of the motivation for exploring the 1-TeV energy scale and of the capabilities of a multi-TeV hadron-hadron collider see, for example, E. Eichten, I. Hinchliffe, K. Lane and C. Quigg, Supercollider Physics, *Rev. Mod. Phys.* **56** (1984) 579 and **58** (1986) 1065.

3. Report of the Ad Hoc Committee on SSC Physics, SSC-250, December 1989.

4. Report of the 1990 HEPAP Subpanel on SSC Physics, DOE/ER-0434, January 1990.

5. Decision Memorandum on the SSC Aperture, R. F. Schwitters, January 1990.

6. Report of the SSC Machine Advisory Committee, December 1989.

7. Possible Scenario to Reach Higher Luminosity, A. Chao, SSC-N-684, November 1989.

8. Report of the DOE Review Committee on the Site-Specific Conceptual Design of the Superconducting Super Collider, to be published by the U.S. Department of Energy.

List of Illustrations

Figure 1.1 A schematic layout of the SSC. 2

Figure 2.1.1 The particles of the standard model. 4

Figure 2.2.1 Interaction of proton constituents. Here a quark from one proton interacts with a quark from another proton. 5

Figure 2.3.1 The invariant mass distribution of Z–boson pairs that would be observed if there is a 400-GeV/c^2 Higgs boson. 6

Figure 2.3.2 The observation of a new neutral gauge boson of mass 4 TeV/c^2. 7

Figure 3.1.1 Luminosity required to produce 100 new Z bosons (Z') in one year 10

Figure 3.1.2 Organization of the SSC Laboratory. 11

Figure 3.2.1 Location of the SSC site. 13

Figure 3.2.2 The SSC footprint 14

Figure 3.2.3 Schematic relationship of the collider tunnel to the geology and topography of the site. 15

Figure 3.2.4 Cross section of the collider tunnel. 16

Figure 4.2.1 Schematic layout of the injector complex. 18

Figure 4.2.2 Schematic arrangement of the lattice components in a superperiod. 21

Figure 4.2.3 Location of the magnets in a typical arc half-cell. 22

Figure 4.2.4 Schematic view of a utility straight section. 22

Figure 4.2.5 Schematic view of the injector complex. 23

Figure 4.2.6 Schematic layout of the major components of a collider dipole cold mass. 28

Figure 4.2.7 Cross section of a collider dipole magnet in the cryostat. 29

Figure 4.2.8 A composite series of training curves for recent long (17 m) R&D collider dipoles. 31

Figure 4.2.9 Schematic view of the computer architecture for the control system. 35

Figure 4.3.1 Schematic layout of the model of experimental halls used to determine experimental support requirements. 37

Figure 4.3.2 Elevation view of a low-b* interaction region. 40

Figure 4.3.3 Exploded view of the Large Solenoid Detector showing major components. 41

Figure 4.3.4 Isometric view of a Type A underground hall. 41

Figure 4.3.5 Isometric view of a Type B underground hall..... 42

Figure 4.3.6 Schematic view of the layout of the test beam area. 43

Figure 4.3.7 A plan view of the test beam optics layout. 44

Figure 5.1.1 The filling sequence from the low-energy booster to the collider

(a) general, (b) more detailed look at the relevant times..... 46

Figure 5.2.1 The diamond bypass arrangement..... 47

Figure 5.2.2 Collider luminosity, beam intensity, and emittance as a function of time..... 48

Figure 5.2.3 Luminosity of the collider assuming a total head-on beam-beam tune shift of 0.01 and a long-range beam-beam limit of 0.005 for each of two high-luminosity regions..... 50

Figure 6.3.1 The SSC construction schedule..... 54

List of Tables

Table 4.2.1 Key parameters of the collider 19

Table 4.2.2 Parameters of the collider ring and the injector complex accelerators 20

Table 4.2.3 Parameters of the high-energy booster 24

Table 4.2.4 Parameters of the medium-energy booster 25

Table 4.2.5 Parameters of the low-energy booster 26

Table 4.2.6 Parameters of the linac 27

Table 4.2.7 Tolerances for the collider dipole multipoles 30

Table 4.2.8 Parameters of NbTi superconducting wire for the SSC magnets 32

Table 4.2.9 Superconducting magnets required for the SSC accelerators 32

Table 4.2.10 Cryogenic system parameters 33

Table 4.2.11 The number of monitor and control points in the accelerator complex 35

Table 4.3.1 Schedule through 1991 for determining the initial SSC experimental program 38

Table 4.3.2 Categories of possible SSC experiments used in estimating experimental hall size and support systems requirements. 39

Table 4.3.3 Dimensions of model underground halls. 42

Table 5.1.1 Cycle times for the injector and the collider 45

Table 5.2.1 Beam parameters that influence luminosity at the design luminosity of 10^{33} cm^{-2} sec^{-1} 48

Table 5.2.2 Parameters for three possible collider operating scenarios 49

Table 6.3.1 Major project milestones 53